CONTENTS

ABSTRACT		i	/A4
PREFACE		iv	1/A7
SUMMARY		1	1/A8
RESEARCH PROGRESS		3	1/A10
I.	FRACTURE MECHANICS INVESTIGATIONS		
	A. J-R Curve Trends of Irradiated, Low Shelf Weld Metal	3	1/A10
II.	FATIGUE CRACK PROPAGATION IN LWR MATERIALS		
	A. Results of Cyclic Crack Growth Rate Studies in Pressure Vessel and Piping Steels	14	1/B13
	B. Corrosion Fatigue Crack Growth Behavior of Pressure Vessel Steels	36	1/D11
III.	RADIATION SENSITIVITY AND POSTIRRADIATION PROPERTIES RECOVERY		
	A. Evaluation and Comparison of IAEA Coordinated Program Steels and Welds with 288°C Irradiation	50	1/E12
	B. Radiation Resistance of A508 Class 2 Forging Steels	60	1/G3
REFERENCES		64	1/G9

MAR 1 0 1981

Y3.N88:25/1783

ORIGINAL

NUREG/CR 1783
NRL Memorandum Report 4400

COMPLETED

Structural Integrity of Water Reactor Pressure Boundary Components

Quarterly Progress Report, April-June 1980

F. J. Loss, Editor

Thermostructural Materials Branch
Material Science and Technology Division

February 20, 1981

Prepared for U.S. Nuclear Regulatory Commission, Office of Nuclear Regulatory Research, Division of Reactor Safety, under Interagency Agreement RES-79-103.

NAVAL RESEARCH LABORATORY
Washington, D.C.

Approved for public release; distribution unlimited.

(72)

NOTICE

This report was prepared as an account of work sponsored by an agency of the United States Government. Neither the United States Government nor any agency thereof, of any of their employees, makes any warranty, expressed or implied, or assumes any legal liability or responsibility for any third party's use, or the results of such use, of any information, apparatus, product or process disclosed in this report, or represents that its use by such third party would not infringe privately owned rights.

The views expressed in this report are not necessarily those of the U. S. Nuclear Regulatory Commission.

Available from

GPO Sales Program
Division of Technical Information and Document Control
U. S. Nuclear Regulatory Commission
Washington, D. C. 20555

and

National Technical Information Service
Springfield, Virginia 22161

SECURITY CLASSIFICATION OF THIS PAGE *(When Data Entered)*

REPORT DOCUMENTATION PAGE

READ INSTRUCTIONS BEFORE COMPLETING FORM

1. REPORT NUMBER NUREG/CR-1783 NRL Memorandum Report 4400	2. GOVT ACCESSION NO.
3. RECIPIENT'S CATALOG NUMBER	
4. TITLE *(and Subtitle)* STRUCTURAL INTEGRITY OF WATER REACTOR PRESSURE BOUNDARY COMPONENTS, QUARTERLY PROGRESS REPORT, APRIL - JUNE 1980	5. TYPE OF REPORT & PERIOD COVERED Progress report on a continuing NRL problem.
	6. PERFORMING ORG. REPORT NUMBER
7. AUTHOR(s) F. J. Loss, Editor	8. CONTRACT OR GRANT NUMBER(s) NRC-RES-79-103 FIN B5528 B&R 60191103
9. PERFORMING ORGANIZATION NAME AND ADDRESS Naval Research Laboratory Washington, D.C. 20375	10. PROGRAM ELEMENT, PROJECT, TASK AREA & WORK UNIT NUMBERS 63-1065-0-1
11. CONTROLLING OFFICE NAME AND ADDRESS U.S. Nuclear Regulatory Commission Division of Reactor Safety Research Washington, D.C. 20555	12. REPORT DATE February 20, 1981
	13. NUMBER OF PAGES 70
14. MONITORING AGENCY NAME & ADDRESS*(if different from Controlling Office)*	15. SECURITY CLASS. *(of this report)* UNCLASSIFIED
	15a. DECLASSIFICATION/DOWNGRADING SCHEDULE

16. DISTRIBUTION STATEMENT *(of this Report)*

Approved for public release; distribution unlimited.

17. DISTRIBUTION STATEMENT *(of the abstract entered in Block 20, if different from Report)*

18. SUPPLEMENTARY NOTES

Prepared for the U.S. Nuclear Regulatory Commission, Office of Nuclear Regulatory Research, Division of Reactor Safety, under Interagency Agreement RES-79-103.

NRC Distribution Category R5 and AN.

19. KEY WORDS *(Continue on reverse side if necessary and identify by block number)*

A533-B submerged arc weld	Irradiated steel	Single specimen compliance test
Charpy V-test	J-integral, R-curve	
Elastic-plastic fracture	Low upper shelf	
Corrosion fatigue	Nuclear pressure vessel steels	
Fatigue crack propagation	Radiation sensitivity	

20. ABSTRACT *(Continue on reverse side if necessary and identify by block number)*

This report describes progress in a continuing program to characterize material properties performance with respect to structural integrity of light water reactor pressure boundary components. Progress under fracture mechanics highlights J-R curve trends from low upper shelf A533-B weld deposits irradiated under the HSST program. Fatigue crack growth rates are being determined for a variety of pressure vessel and piping steels in simulated nuclear coolant environments. Three regions of crack growth behavior which have been associated with classical stress corrosion cracking and corrosion fatigue now have been clearly defined for reactor vessel steels. A theory of the influence of dissolved oxygen content in the fatigue crack growth in simulated PWR coolant is

(Continues)

20. Abstract (Continued)

proposed. Work in radiation sensitivity describes recent progress in radiation studies involving reactor vessel steels in a coordinated IAEA program. Also reported is a notch ductility characterization of A508-2 forging steel with irradiation.

CONTENTS

ABSTRACT i

PREFACE iv

SUMMARY 1

RESEARCH PROGRESS 3

I. FRACTURE MECHANICS INVESTIGATIONS

A. J-R Curve Trends of Irradiated, Low Shelf Weld Metal 3

II. FATIGUE CRACK PROPAGATION IN LWR MATERIALS

A. Results of Cyclic Crack Growth Rate Studies in Pressure Vessel and Piping Steels 14

B. Corrosion Fatigue Crack Growth Behavior of Pressure Vessel Steels 36

III. RADIATION SENSITIVITY AND POSTIRRADIATION PROPERTIES RECOVERY

A. Evaluation and Comparison of IAEA Coordinated Program Steels and Welds with 288°C Irradiation 50

B. Radiation Resistance of A508 Class 2 Forging Steels 60

REFERENCES 64

PREFACE

The goal of this research program is to characterize materials behavior in relation to structural safety and reliability of pressure boundary components for light water reactors. Specific objectives include developing an understanding of elastic-plastic fracture and corrosion fatigue crack propagation phenomena in terms of continuum mechanics, metallurgical variables, and neutron irradiation. Emphasis is placed on identifying metallurgical factors responsible for radiation embrittlement of steels and on developing procedures for embrittlement relief, including guidelines for radiation resistant steels. The underlying objective is the interpretation of material properties performance to establish engineering criteria for structural reliability and long term operation. Current work is organized into three major tasks: (1) fracture mechanics investigations, (2) fatigue crack propagation in high-temperature, primary reactor water, and (3) radiation sensitivity and postirradiation properties recovery. A part of the corrosion fatigue tests in Task 2 is being performed under subcontract to the Westinghouse Electric Corporation. This work is being coordinated with on-going research of a similar nature at NRL to form a uniform program having common objectives.

This work is being performed at NRL by the Material Science and Technology Division, Thermostructural Materials Branch, F. J. Loss, program manager. NRC funding is provided by the Office of Nuclear Regulatory Research, Metallurgy and Materials Research Branch, Milton Vagins, project manager.

STRUCTURAL INTEGRITY OF WATER REACTOR PRESSURE BOUNDARY COMPONENTS QUARTERLY PROGRESS REPORT, APR-JUN 1980

SUMMARY

I. FRACTURE MECHANICS INVESTIGATIONS

A. J-R Curve Trends of Irradiated, Low Upper Shelf Weld Metal

J-R curves have been developed from two A533-B submerged arc weld deposits. These welds were irradiated in the HSST program and have postirradiation Charpy-V upper shelf energies of 68 and 81J, respectively. The 1.6T-CT specimens from this program were characterized by the single specimen compliance technique and represent the largest irradiated specimens ever tested in this manner. The initial portion of the R curve can be described by a power law behavior. This confirms the trend for reactor vessel steels observed with smaller specimens and which was first disclosed by the authors in previous progress reports of this series. At larger crack extensions the R curve flattens so that a power law description is unconservative. In fact, a tearing modulus T of essentially zero was computed at the point of test termination. However, the specimens were taken to long crack extensions, greater than one-third of the original unbroken ligament, which may have caused the crack to outgrow the region of J dominance and thus possibly invalidate the computed values of J and T. Planned tests of larger (4T-CT) specimens of these welds will provide information to assess the validity of the current results at large values of crack extension.

II. FATIGUE CRACK PROPAGATION IN LWR MATERIALS

A. Results of Cyclic Crack Growth Rate Studies in Pressure Vessel and Piping Steels

Fatigue crack growth rate (FCGR) data from unirradiated A508-2 steel from two heats is compared. FCGR data from a series of 1 Hz sinusoidal waveform tests of both irradiated and companion unirradiated specimens of A533-B and A508 is also presented. Irradiation damage does not seem to influence the data, which was produced for a load ratio of 0.2 and a simulated PWR coolant environment. Test results for A106 Grade C piping steel are also included and exhibit growth rates slightly lower than those normally expected for the selected test parameters (17 mHz sinusoidal waveform, R = 0.2).

The existence of three regions in the crack growth rate plots has been noted. These three regions have been described by many authors for tests of other structural steels in other environments but have never before been clearly identified for RPV steels in PWR environments. The three regions are the result of the varying degrees of interaction of the specimen with the environment and their location is a function of the material, environment, and load waveform parameters. A theory of the influence of dissolved oxygen content on the fatigue crack growth results in simulated PWR coolant is proposed.

Manuscript submitted December 5, 1980.

B. Corrosion Fatigue Crack Growth Behavior of Pressure Vessel Steels

Testing continues in accordance with the matrix being executed jointly by Westinghouse and NRL. Fatigue crack growth rates have been found to be equal or lower in welds than in the corresponding base metals. In addition, it appears that there can be significant differences in the susceptibility of different materials to water reactor environments, and the degree of susceptibility may be a function of the sulfur content of the steel. Specifically, it appears that low sulfur steels may display environmental fatigue crack growth which is only slightly accelerated over air behavior.

Static load stress corrosion cracking tests are continuing on base metals as well as welds and heat-affected zones. Static crack extension has been found in two separate heat-affected zones, but none has been observed in base metal or welds. Two additional heat-affected zones are being added to those under test, to better characterize the observed behavior.

III. RADIATION SENSITIVITY AND POSTIRRADIATION PROPERTIES RECOVERY

A. Evaluation and Comparison of IAEA Coordinated Program Steels and Welds With 288°C Irradiation

The dynamic fracture toughness properties of four steel materials supplied by France and the FRG to the IAEA Program on "Analysis of the Behavior of Advanced Reactor Pressure Vessel Steels Under Neutron Irradiation," were established during this period. Comparisons were made against parallel determinations for materials supplied by Japan. Significant differences in 100 MPa $\sqrt{m}$ transition temperatures were observed; however, a high upper shelf toughness was exhibited by all eight materials.

B. Radiation Resistance of A508 Class 2 Forging Steels

The detrimental effects of neutron irradiation on the notch ductility and dynamic fracture toughness of commercially produced A508 Class 2 forgings are being assessed using C_v and PCC_v test methods. Initial results for one forging irradiated in two reactor assemblies to $\sim 2.8 \times 10^{19}$ n/cm^2, E>1 MeV, indicate a high resistance to radiation effects and a good reproducibility of experimental results. The two test methods also show good agreement in their individual assessments of the radiation effect on fracture resistance.

RESEARCH PROGRESS

I. FRACTURE MECHANICS INVESTIGATIONS

A. J-R Curve Trends of Irradiated, Low Upper Shelf Weld Metal

F.J. Loss, B.H. Menke, A.L. Hiser, and H.E. Watson

INTRODUCTION

Previous studies have shown that A533-B submerged arc weld deposits of the type used in the beltline region of some commercial, light water reactors can exhibit low Charpy-V (C_v) upper shelf energy levels after irradiation, that is, energy levels which lie below 68J (50 ft-lb) [1,2]. In view of this behavior emphasis in research programs has been placed upon characterizing the fracture toughness of these steels in order to provide a quantitative basis to assess the margin of safety during reactor operation. The objective of the current fracture toughness program is to develop J-R curve trends within the upper shelf regime. It is believed that these data could be used in conjunction with a tearing instability concept as defined by Paris [3] to assess the margin of safety against catastrophic fracture.

As part of the Heavy Section Steel Technology (HSST) Program seven A533-B submerged arc weld deposits (61W-67W) have been irradiated [4] to provide a source of materials having low, upper shelf energy. Compact toughness (CT) specimens of various sizes, which include 0.5T-, 0.8T-, 1.6T-, and 4T-CT as well as C_v specimens were irradiated in this program to nominal fluence levels of 0.6 to 1.8 x 10^{19} n/cm^2 >1 MeV; postirradiation C_v upper shelf energy levels for these welds ranged from 54 to 81J (40 to 60 ft lb) [1,5]. Initial testing of the 0.5T-CT specimens has been accomplished through a coordinated program between NRL and the Hanford Engineering Development Laboratory [6,7]. The remaining specimens from these irradiations are being tested by NRL. The first J-R curve results from the irradiated 1.6T-CT specimens are presented here.

EXPERIMENTAL APPROACH

J-R curves have been obtained by means of the single specimen compliance (SSC) technique that was described in previous reports [8,9]. This method is capable of producing well-defined R curves having little scatter among the data points. In addition, it has been found that the crack extension must proceed uniformly throughout the specimen thickness in order to achieve an accurate correspondence between this quantity as predicted by the SSC technique and as measured optically after the specimen has been broken apart [9]. Previous studies by the authors have shown that side grooving of the specimen by 20 percent is required to achieve a straight crack-front extension in nuclear vessel steels. In this regard, the initial tests of irradiated 0.5T-CT specimens from the subject welds using 10% side grooves [6,7] showed that extensive crack-front tunneling resulted as the R curves were developed. Consequently, a side-groove depth of 20% was chosen for the 1.6T-CT tests of these same steels.

RESULTS

The first R curves from the 1.6T-CT HSST specimen irradiations are shown in Fig. 1. Test details are given in Table 1. The two weld deposits, 61W and 62W, represent C_v upper shelf energies of 68 and 81J (50 and 60 ft lb), respectively. The test temperature of 200°C was chosen to be on the C_v upper shelf for both materials. The crack extension (Δa) was purposely taken to large values e.g., 14 to 20 mm, in that this had never before been accomplished for irradiated vessel steels. Even at this long crack extension the crack front profile remained straight (Fig. 2) and the correspondence between measured and predicted values of final crack extension was excellent.

The R curves in Fig. 1 have been corrected for crack extension using the relationship derived by Ernst and Paris [10]:

$$J_{i+1} = \left[J_i + \left(\frac{\eta}{b}\right)_i \frac{A_{i,\,i+i}}{B_N} \right] \left[1 - \left(\frac{\gamma}{b}\right)_i (a_{i+1} - a_i) \right] \qquad (1)$$

where $\eta = 2 + 0.522\ b/W$
$\gamma = 1 + 0.76\ b/W$
b = unbroken ligament
W = width
A = area under load vs load-line displacement record
a = crack length
B_N = net specimen thickness

As seen in Fig. 3, this correction is not large at small values of crack extension but it can be quite significant for crack extension increments of 5 mm or more.

Expanded R curves for $\Delta a < 1.5$ mm are presented in Figs. 4 and 5. These curves highlight the power law behavior exhibited at small values of crack extension. The latter has been discussed in previous progress reports [9] where it was first documented by the authors. It has been found convenient to fit the initial portion of the R curve with the form:

$$J = C\ \Delta a^n \qquad (2)$$

where C and n are fitted constants and Δa is the crack extension. The formulation is indicated in Figs. 4 and 5. Because of this curvature in the R curve, it is not possible to define a unique value of tearing modulus T for these materials. For comparison between different steels, however, we have defined an average value of T which characterizes the R curve for a limited crack extension increment of $0.15 < a < 1.5$ mm (Table 1).

As explained in Ref. 9, the power law behavior led the authors to devise a new definition of J_{Ic} which allows a small amount of crack extension. Specifically, J_{Ic} is computed from the power law fit at a point where the R curve crosses the 0.15 mm extension line. This definition J_{Ic} is different from that of the proposed ASTM procedure for J_{Ic}. However, the ASTM procedure was designed for multiple specimen testing whereby the curvature in the R curve for nuclear vessel steels cannot be readily discerned. Consequently, J_{Ic} by the latter procedure is taken as the intersection of the least squares fit to the data between the exclusion lines in Fig. 4 and the blunting line. As shown in Table 1, the agreement in J_{Ic} by these two

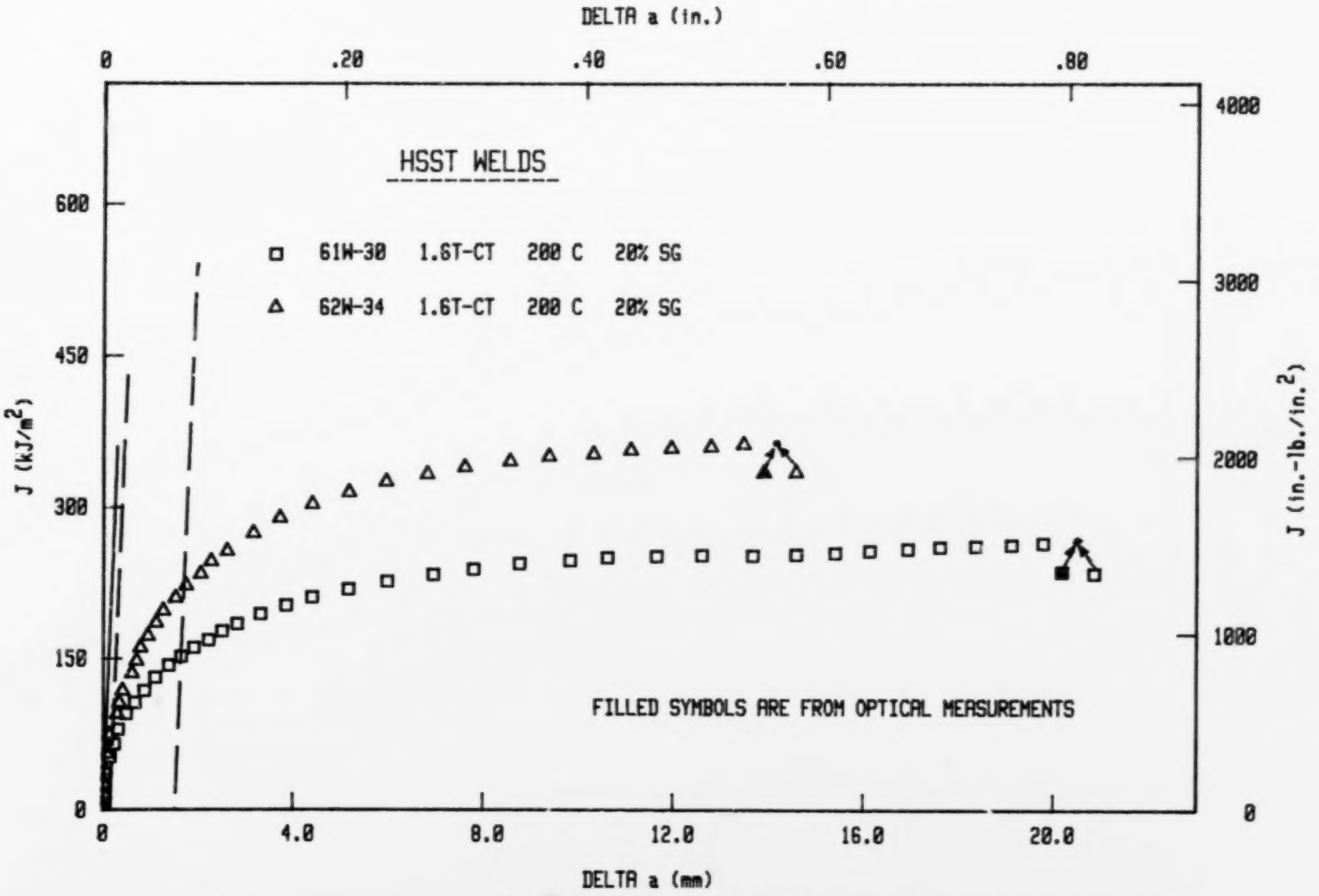

Fig. 1 - J-R curves from A533-B submerged arc weld deposits which were irradiated in the HSST program. The fluence levels are 12 and 16 x 10^{18} n/cm^2 > 1 Mev for welds 61W and 62W, respectively.

TABLE 1 - Fracture Toughness Properties

Specimen No.	CT Size	% Side Grooves	Fluence $\times 10^{18}$ >1 MeV	Test Temp. ^{o}C	$\left(\frac{a}{W}\right)_i$	a_i mm	C_v Shelf J
61W-30	1.6	20	12	200	0.535	37.7	68-72
62W-34	1.6	20	16	200	0.519	39.0	79-81
62W-100	0.5	10	13	176	0.511	12.2	79-81

Specimen No.	J_{Ic}[a] kJ/m^2		K_{Jc}[b]	T_{AVG}[c]	at $\Delta a = 1.5$ mm		at $\Delta a = 6$ mm	
	NRL	ASTM	$MPa\sqrt{m}$		T	ω	T	ω
61W-30	61	61	115	31	22	9	5	1.2
62W-34	88	83	137	45	31	10	6	1.1
62W-100	101	97	147	38	24	2	-	-

[a] As defined (1) by NRL and (2) by the proposed ASTM J_{Ic} standard

[b] $K_{Jc} = \left[EJ_{Ic}/(1-\nu^2)\right]^{1/2}$

[c] Averaged between $0.15 < \Delta a < 1.5$ mm

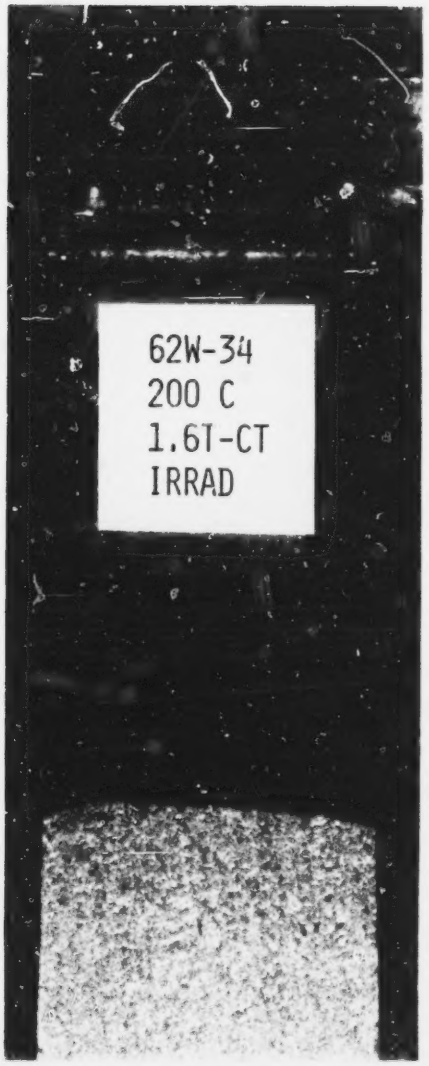

Fig. 2 - Fracture surface of irradiated 1.6T-CT specimen illustrating the straight crack front extension. The specimen was side grooved by 20%.

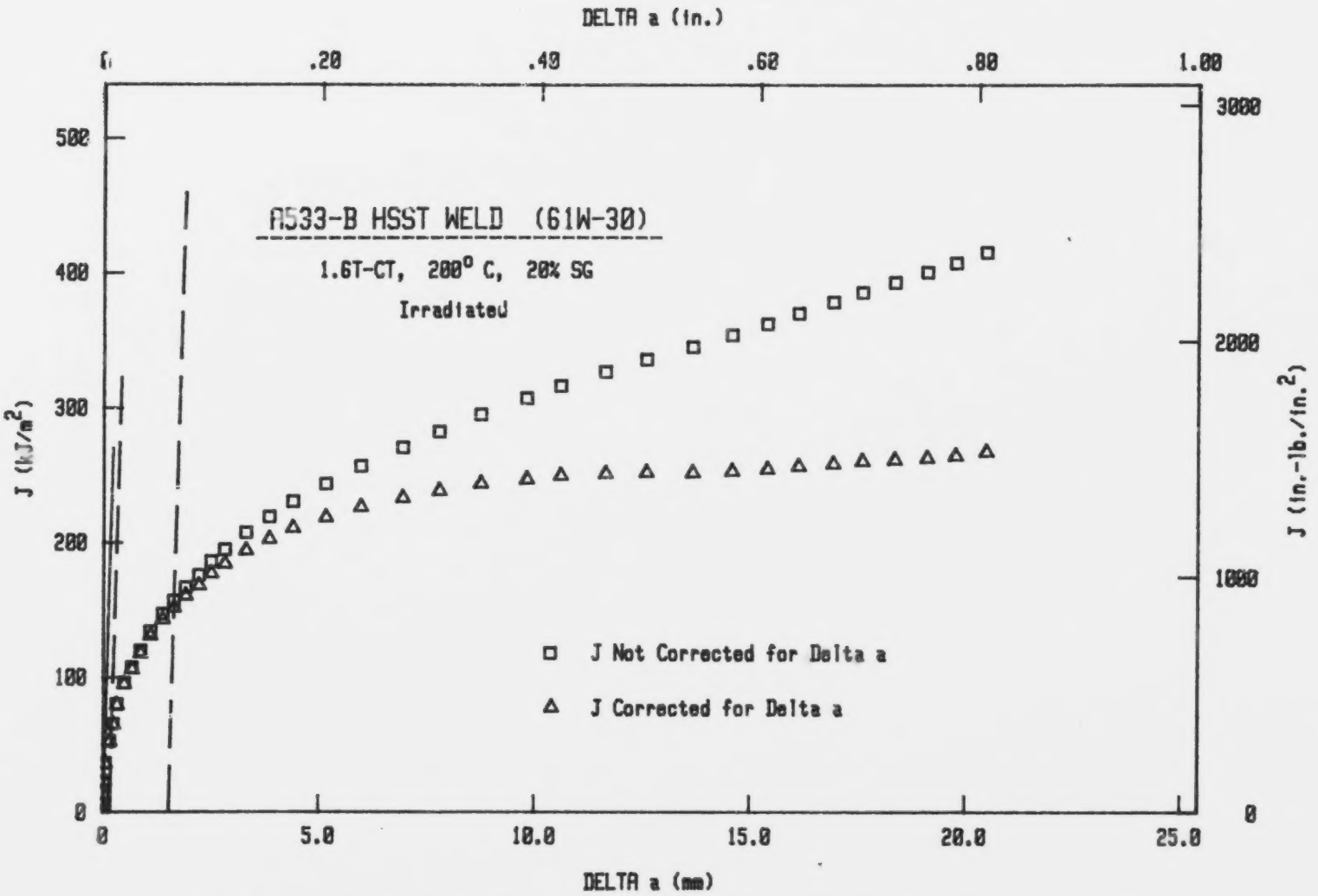

Fig. 3 - J-R curve for irradiated 1.6T-CT specimen illustrating the significance of the correction to J for crack extension.

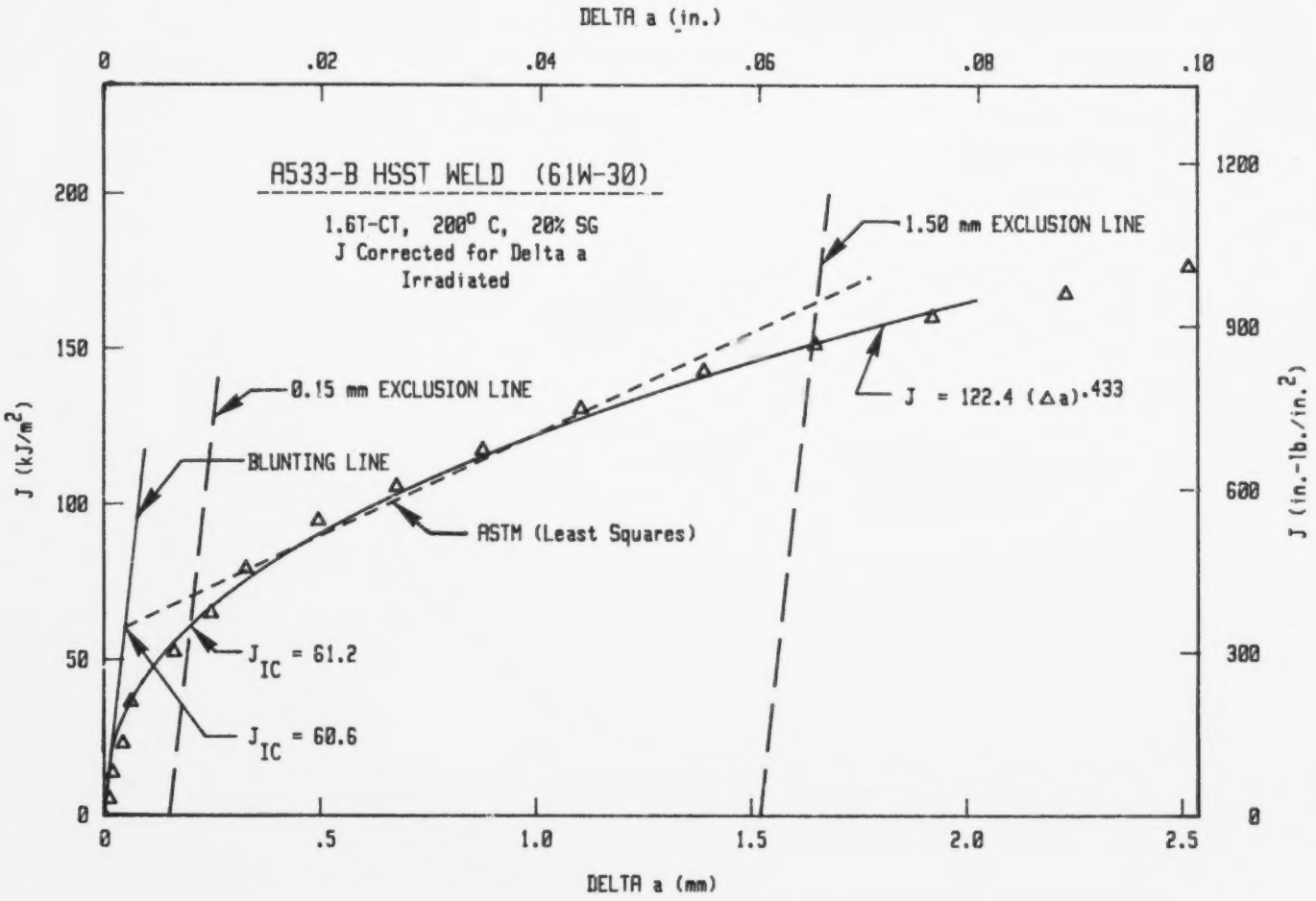

Fig. 4 - Expansion of the R curve of Fig. 1 illustrating the power law behavior exhibited at small crack extension. With the NRL procedure, J_{IC} is taken as that value where the R curve intersects the 0.15 mm exclusion line. Conversely, J_{IC} is defined by the proposed ASTM standard as the intersection of the least squares fit of the data (between exclusion lines) with the blunting line.

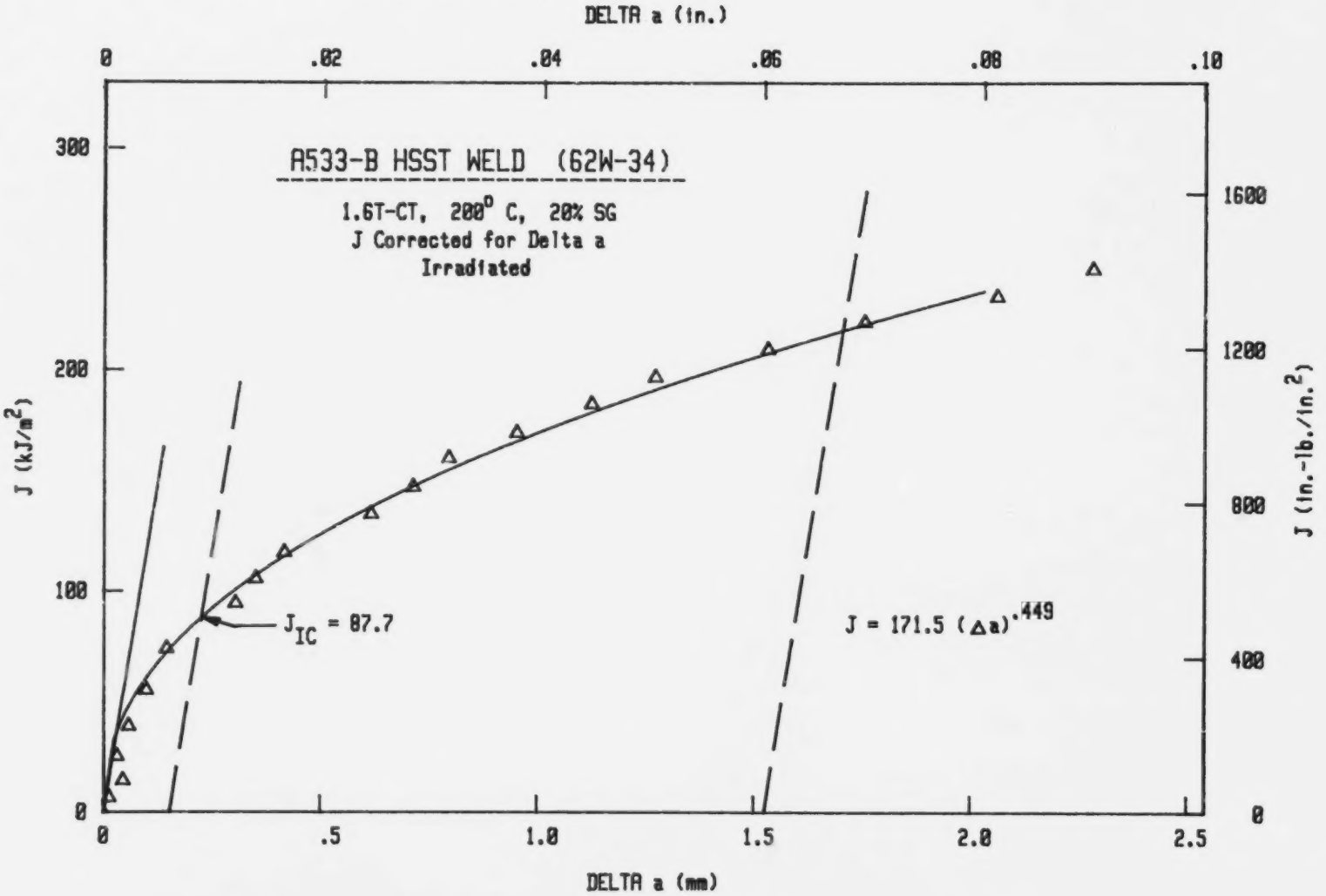

Fig. 5 - Expansion of the J-R curve illustrated in Fig. 1 showing the power law behavior of the R curve for small values of crack extension.

procedures in quite good. In addition, the J_{Ic} values in Table 1 are "valid" according to the criteria contained in the proposed ASTM J_{Ic} standard. These values have been used to compute K_{Jc} from the relationship:

$$K_{Jc} = \left[\frac{EJ_{Ic}}{(1-\nu^2)}\right]^{1/2} \quad (3)$$

where E and ν are Young's modulus and Poisson's ratio, respectively (Table 1). For the weld having a 68J upper shelf energy, K_{Jc} is 115 MPa$\sqrt{m}$ (104 ksi$\sqrt{in}$).

It should be noted that the power law expression of the data in Figs. 4 and 5 cannot be extrapolated beyond the region shown; the flattening of the R curve at large crack extensions precludes an accurate fit of the data by a power law formulation. In fact, the value of the tearing modulus is essentially zero at the point where the test was terminated. As shown in Fig. 6, extrapolation of this equation can lead to large errors in J.

Figure 7 compares R curves from weld 62W generated by two different size specimens, 0.5T- and 1.6T-CT. (The result for the 0.5T-CT test is described in Ref. 6.) The irradiation conditions and test temperatures for both specimens were similar. While the R curves for these specimens are identical at small values of crack extension, the curve for the 0.5T-CT specimen appears to project a lower trend at Δa values greater than 1.5 mm. Since the 0.5T-CT specimen exhibited tunneled crack extension it was expected that its R curve would lie above, and not below, that of the 1.6T-CT specimen. Previous studies [9] have shown that for the same size specimens, crack-front tunneling produces an R curve which lies above that associated with a straight crack-front extension.

Validity Criteria

There currently exist no formal validity criteria for the R curves in Fig. 1. Hutchinson and Paris [11] have suggested that $\omega \gg 1$ for validity where $\omega = (b/J)(dJ/da)$. Additionally, Shih [12] has suggested a "J dominated" region limited to crack extension increments less than 6% of the unbroken ligament (0.06b). In this region the strain field characterized by J is not substantially influenced by the magnitude of the crack extension. For the results shown in Fig. 1, the latter would restrict the crack extension to approximately 2 mm whereas the actual crack extension was almost an order of magnitude greater than this proposed limit. On the other hand, the authors have presented experimental data which show no change in the R curve when the 0.06b criterion is violated by use of a smaller size specimen to the extent that Δa is 20% of the unbroken ligament [13].

With respect to the ω criterion, Table 1 shows ω values of approximately 10 at a crack extension of 1.5 mm for the larger-size specimens; a value of unity is attained at a Δa of approximately 6 mm. From this behavior, one can conclude that the R curves in Fig. 1 satisfy the ω criterion for about one-third of the crack extension shown. This region of presumed validity can be extended only through the use of larger specimens. If the R curve is a material property within the region of validity, then the planned testing of irradiated 4T-CT specimens of the welds indicated in Fig. 1 should provide the means with which to assess the level of ω which must be satisfied by a small specimen to predict the results of a similar but larger specimen.

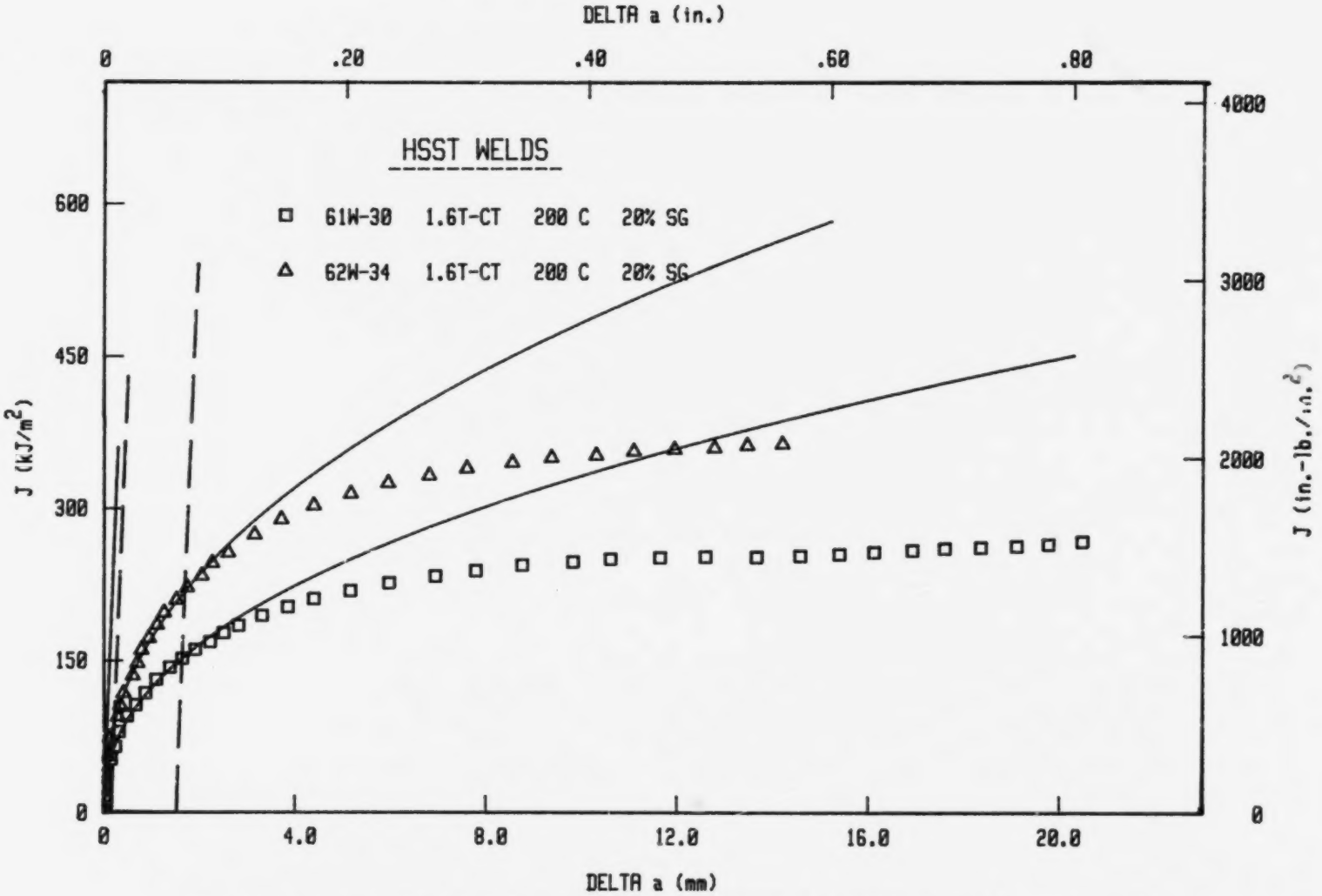

Fig. 6 - Extrapolation of the power law fit illustrated in Figs. 4 and 5. At crack extensions beyond 1.5 mm this formulation can greatly overestimate J well as the tearing modulus. (The latter is dependent upon the slope of the R curve.)

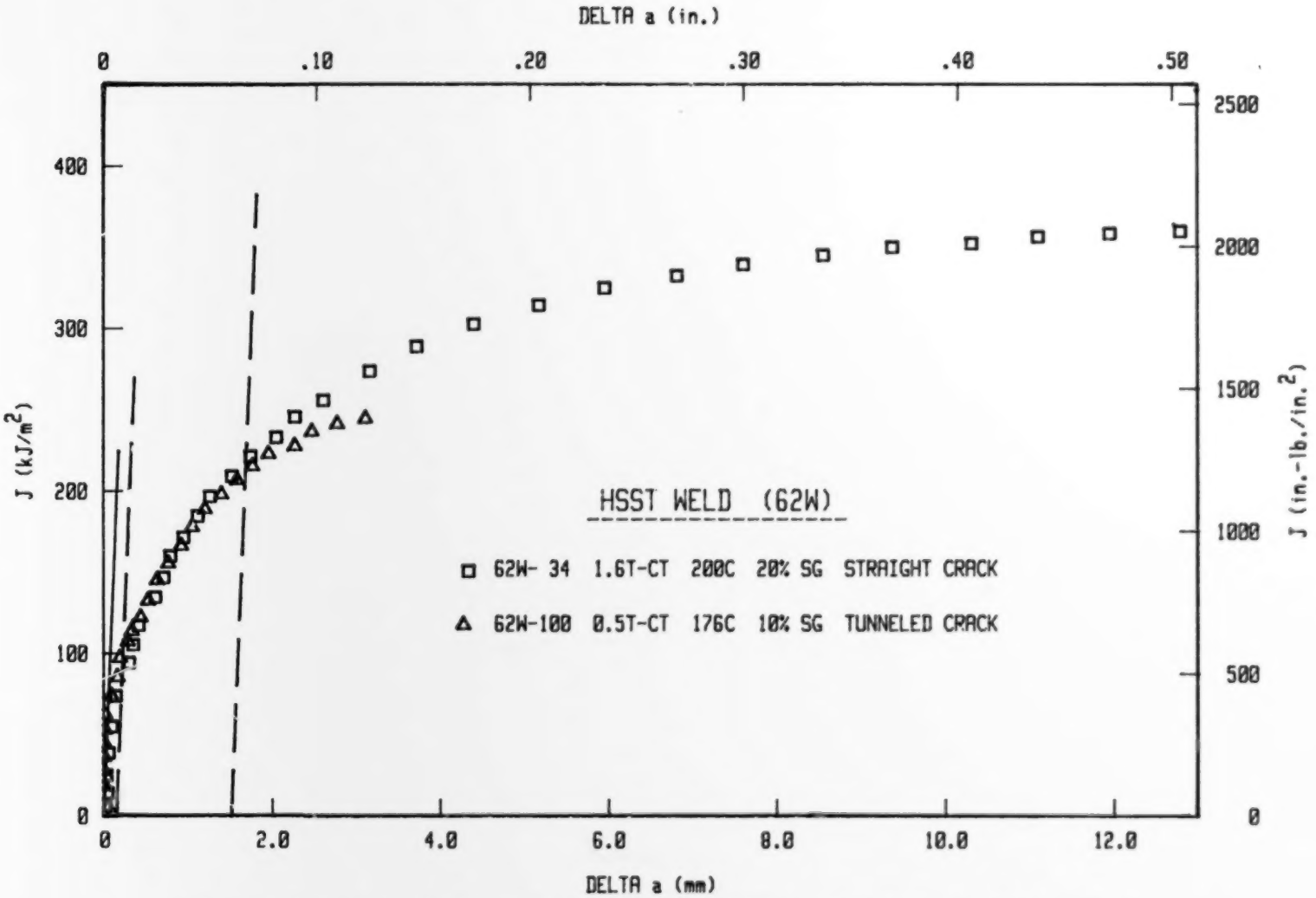

Fig. 7 - Comparison of R curves from Weld 62W with CT specimens of two sizes. A tunneled crack front was exhibited by specimen 62W-100 because the side grooves were of insufficient depth (Ref. 6). The fluence levels for specimens 34 and 100 were 16 and 13 x 10^{18} n/cm^2 >1 MeV, respectively.

II. FATIGUE CRACK PROPAGATION IN LWR MATERIALS

A. Results of Cyclic Crack Growth Rate Studies in Pressure Vessel and Piping Steels

W. H. Cullen, Jr., R. A. Taylor and H. E. Watson

BACKGROUND

The fatigue crack growth rate (FCGR) evaluation program at NRL consists of several efforts which address specific topics of importance to nuclear reactor design, in-service inspection, and continued safe operation. Several tests are being carried out in an environment which simulates the PWR primary-loop, nuclear-core-coolant chemistry using waveforms which describe certain transients and operational changes in reactor pressure which may lead to subcritical extension of pre-existing flaws. These sub-programs are as follows:

a. Main Matrix Tests (Unirradiated) - a test plan aimed at evaluation of fatigue crack growth rates for several reactor pressure vessel steels and welds, including both fused weld metal and heat-affected zones. This program is conducted jointly by NRL and the Westinghouse Nuclear Energy Systems Division under a subcontract.

b. Main Matrix Tests (Irradiated) - this plan is actually a subset of the Main Matrix described above, and includes tests of selected specimens of the same materials as above, but irradiated to total fluences of 2 to 4 x 10^{19} n/cm^2 (>1 MeV). This testing is also carried out in the high-temperature, PWR water environment.

c. Piping Matrix - a test plan in which several piping materials are to be tested in the simulated PWR coolant environment. The waveforms and load ratios for these tests are similar to those selected for the Main Matrix tests.

d. Variable Amplitude/Variable Frequency Test Matrix - a test plan which is carried out in association with the cold leg integrity evaluation. Several specimens of piping materials will be tested in the high-temperature, PWR water environment.

e. Supporting Tests and Extended Analysis of Data - this category includes a variety of tests and theoretical developments which are carried out to assist in the interpretation and application of FCGR data from the above test plans. Additional FCGR tests, mechanical properties studies, stress-corrosion cracking, fractographic, water chemistry and oxide film studies lead to the continued development of models of fatigue crack growth in these materials in the simulated nuclear coolant environment.

TEST STATUS AND PROGRESS

The progress in each of these areas, during the past quarter, and a summary of expected developments is described in the following sections.

a. Main Matrix Tests (Unirradiated)

The status of main matrix tests, both completed and underway, is shown in Table 2. The items tested under the Westinghouse Subcontract are reported and discussed in a separate section. Presently, the NRL has six main matrix (unirradiated) tests underway, and at the end of this quarter, the NRL test status was that shown in Table 3.

Table 2 - Main Test Matrix (Unirradiated Materials)

	R = 0.2		R = 0.5		R = 0.7	
	17 mHz Sinewave	1 min Ramp	17 mHz Sinewave	1 min Ramp	17 mHz Sinewave	1 min Ramp
A508	5C	3C	D	D	1C+U	S+U
A533-B	3C	C+U	D	D	3C	S+U
Submerged Arc Weld Linde 80 - Weld	2C+S	2C	D	D	2C	C+S
Linde 80 - HAZ (In A508-2)	2C	C+S	D	D	C+S	C+S
Linde 0091-Weld	3C	C+S	D	D	U+C	S+U
Linde 0091 - HAZ (In A533-B1)	C	2S	D	D	S+U	2S
Linde 124 - Weld	2C	2C	D	D	2C	2C
Linde 124 - HAZ (In A533-B-1)		C	D	D	S	S

Entries reflect combined Westinghouse and NRL effort.

S - Test scheduled
C - Test completed
D - Test deferred
U - Test underway

Table 3 - Tests in Progress - 30 June 1980 - NRL

Test Stand	Material	Conditions
IT Autoclave	Irradiated Mn-Mo Weld (Linde 0091 Flux)	17 mHz sinewave R = 0.2
2/4T Autoclave	Irradiated A508-2	17 mHz sinewave R = 0.7
Multispecimen No. 1	A533-B Mn-Mo Weld (Linde 0091 Flux)	60 sec. ramp 1 sec. reset R = 0.2
Multispecimen No. 2	A106-C A508-2 A533B Mn-Mo Weld (Linde 0091 Flux)	60 sec. ramp 1 sec. reset R = 0.7
Multispecimen No.3	A508-2 A516 Mn-Mo Weld (Linde 0091 Flux)	17 mHz sinewave R = 0.7

In the previous quarterly report [14], results for a 60 sec. ramp/1 sec reset test of A508-2 forging-code V82 were presented, and comparison of these results with previously obtained results for similar tests on other heats of A508-2 indicated the V82 heat was more susceptible to environmentally-assisted fatigue crack growth. A companion test of this V82 forging, a 17 mHz sinusoidal waveform test, was completed during this quarter. The former results are shown in Fig. 8a, and the most recent results in Fig. 8b. Once more, the code V82 material produced fatigue crack growth rates higher than the R-code material although the differences for the 17 mHz test are considerably less substantial than for the 60 sec ramp test.

b. Main Matrix Tests (Irradiated)

During this quarter, a major, and successful effort was devoted to a scoping study aimed at a delineation of the frequency dependence of the irradiated specimens. Recently tests of both irradiated and companion unirradiated specimens have been carried out at a frequency of 1 Hz over a ΔK range beginning at ~ 13 MPa$\sqrt{m}$. These results, combined with results obtained earlier, are described below.

Data for A533-B steel in both the irradiated and unirradiated condition is shown in Figs. 9a and b. Although the materials (codes L83 and HT) are from different heats, and the initial ΔK for the HT-material tests is somewhat higher, the trend of the results is very similar. The 1 Hz tests produce results residing on or near the ASME air default line over the higher portion of the ΔK range which was tested. The 17 mHz results show a substantial increase in growth rate over the 1 Hz results, but since the increase is about the same for both irradiated and unirradiated material, it appears to be a function of the environment and cyclic period, rather than irradiation. Irradiated specimen L83-1 was tested over a ΔK range which began with a value sufficiently low that the classical-three-region behavior of corrosion fatigue crack-growth rates can be seen [15]. Region I, or start-up behavior occurs at the lowest values of the ΔK range, with crack growth rates rising to a plateau, Region II behavior, characterized by somewhat more ΔK-independent growth rates then for Regions I or III. Lastly, for the higher ΔK values, Region III behavior, the growth resumes a strong ΔK-dependence. In this particular case, the 17 mHz test was terminated before Region III onset had been established. This test was and, in fact, all tests were, deliberately terminated well before fracture of the ligament remaining in the specimen (s) so that a final crack length, as inferred from the LVDT displacement gage, could be optically confirmed from the specimen(s) fatigue fracture surface. The three-region phenomenon is further discussed in Section e(1).

Figure 10 presents the results of an effort to separate, if present, the effect of irradiation time at temperature from the effect of irradiation damage itself. Specimen L83-19 was conditioned at 288^{o}C for 1225 hours which, combined with residence time in the autoclave prior to and during the test, closely approximates the time for irradiations of the other L83 specimens described above. Specimen L83-18 was tested in the as-received condition. Results of 1 Hz tests in reactor-grade water environment of all three specimens (L83-1, -18, -19) are shown in Fig. 10, allowing the conclusion that the response of the material to fatigue is essentially unaltered by irradiation or by an equivalent time at temperature for these materials as evaluated in this study.

A similar set of tests was conducted on A508-2 material, code Q71. These results are shown in Fig. 11. As for A533B, there is a significant increase in growth rates for the 17 mHz waveform as opposed to the 1 Hz waveform, but this increase is nearly identical to the increase shown in Fig. 9a, b and as before, is due to the influence of the environment during the longer period waveform. Since the test on Q71-9 was

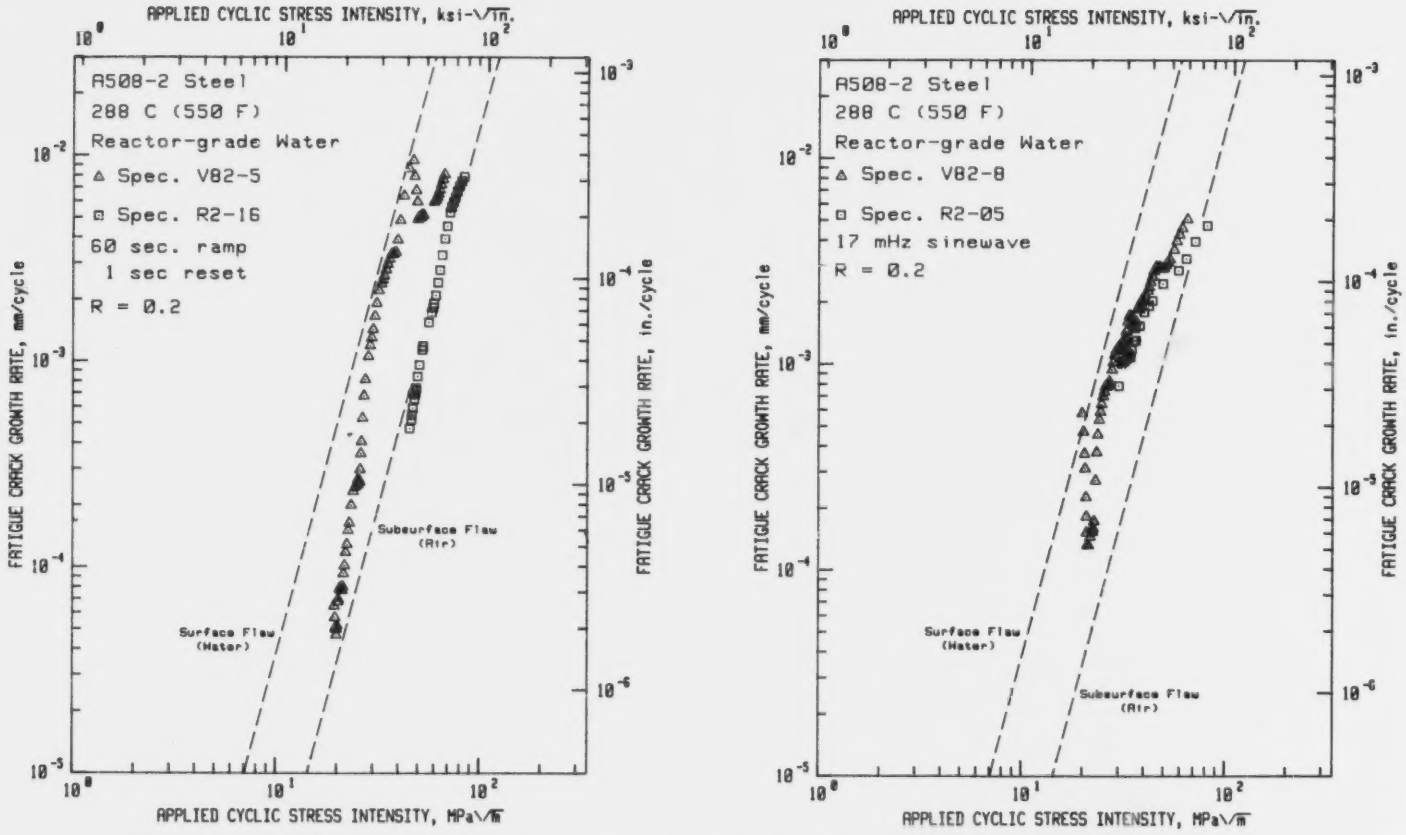

Fig. 8 - Fatigue crack growth rates vs applied cyclic stress intensity factor for unirradiated, as-received A508-2 steel in high-temperature, pressurized reactor-grade water. The code V82 heat shows slightly more susceptibility to corrosion fatigue crack growth, as shown in Fig. 8a, for 60 sec ramp/1 sec reset waveforms and Fig. 8b, for 17 mHz sinusoidal waveforms.

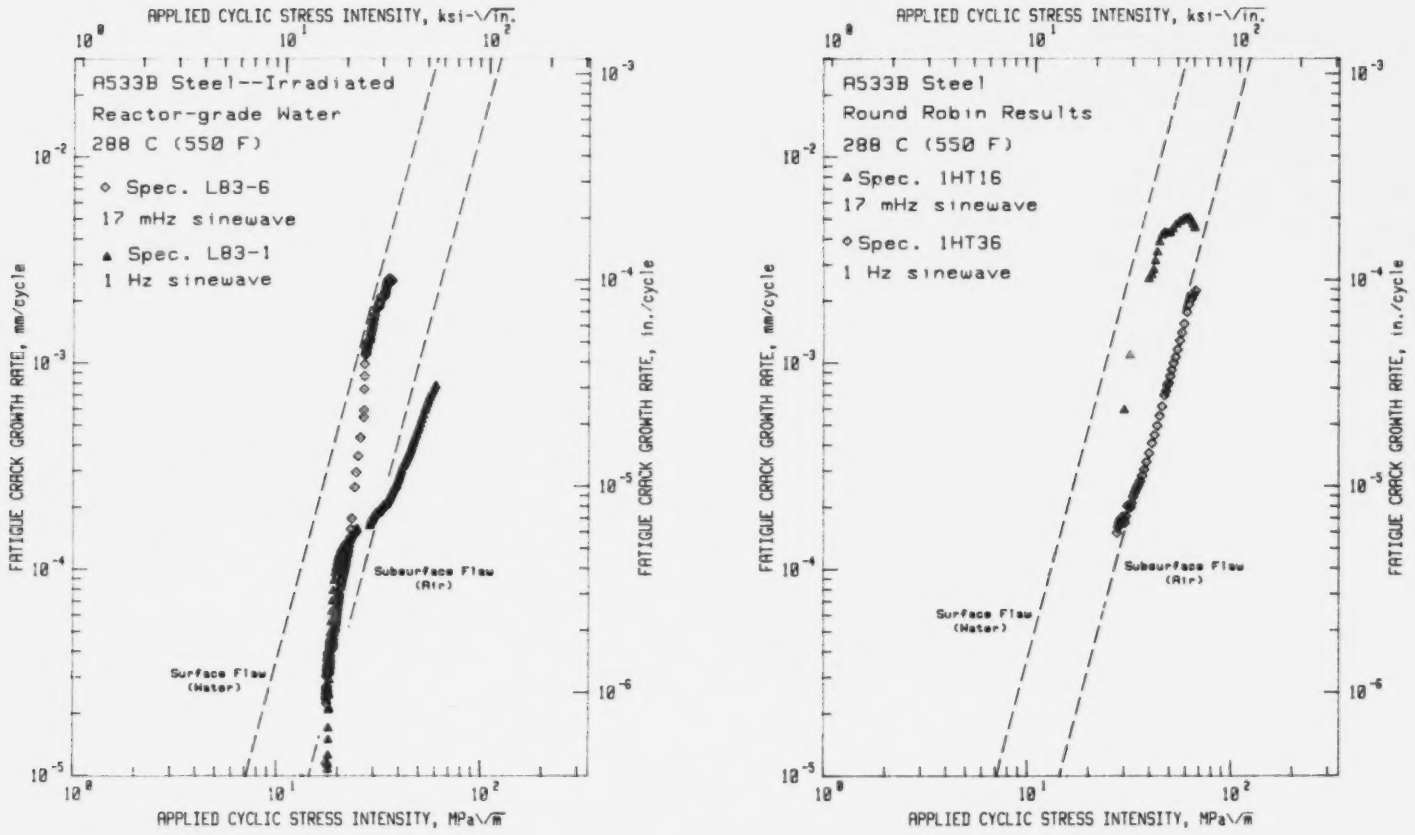

Fig. 9 - Fatigue crack growth rates vs applied cyclic stress intensity factor for (a) irradiated and (b) unirradiated A533B steel in high-temperature pressurized reactor grade water. Comparison of these two graphs shows the parallel behavior of the irradiated and unirradiated specimens. Since the unirradiated tests began at a rather high initial value of ΔK, the three-stage behavior, seen clearly in irradiated specimen L83-1, does not manifest itself. Specimens L83-1 and L83-6 were irradiated to a total fluence of 3.4×10^{19} n/cm^2 > 1 MeV.

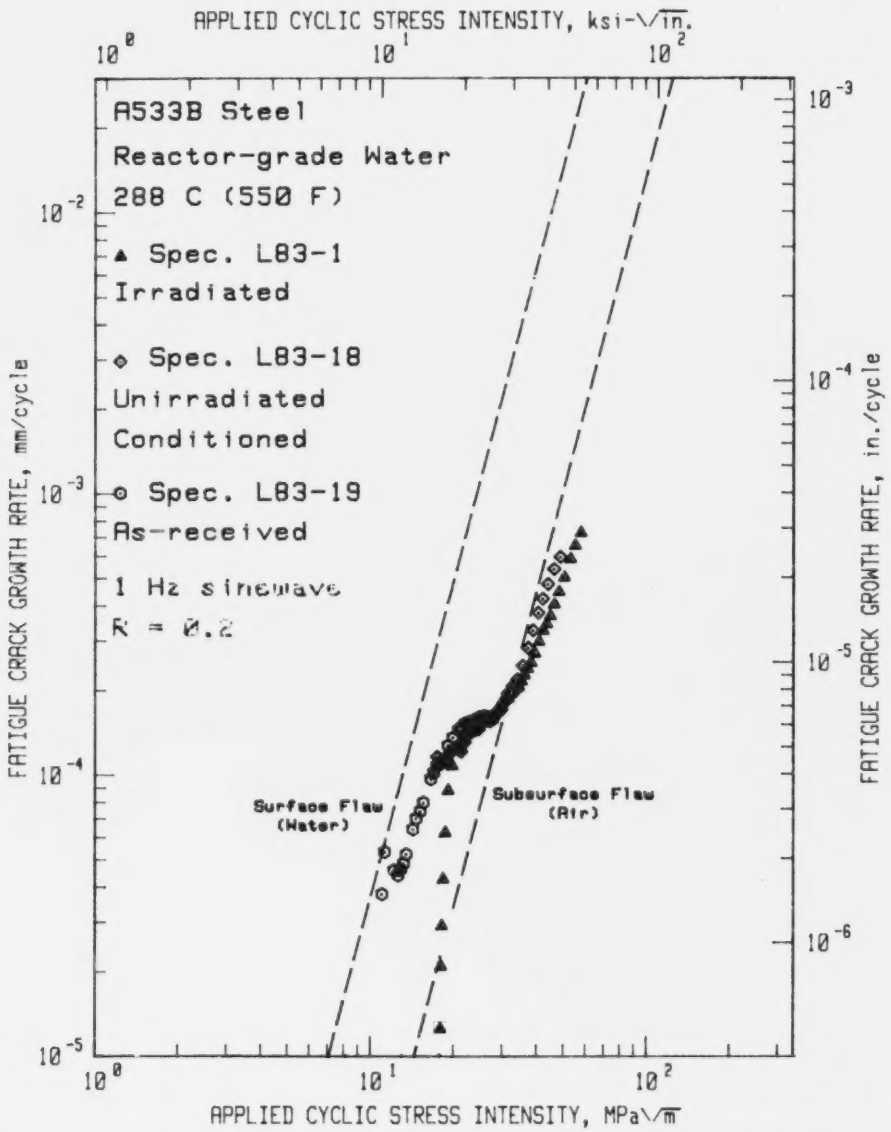

Fig. 10 - Fatigue crack growth rates vs applied cyclic stress intensity factor for (a) as-received, (b) unirradiated, but conditioned at reactor time and temperature, and (c) irradiated A533-B steel in high-temperature, pressurized reactor-grade water. These three overlapping data sets indicate that irradiation, under conditions of this initial study, has an essentially insignificant effect on fatigue crack growth rate. Specimen L83-1 was irradiated to a total fluence of 3.4×10^{19} n/cm^2 > 1 MeV.

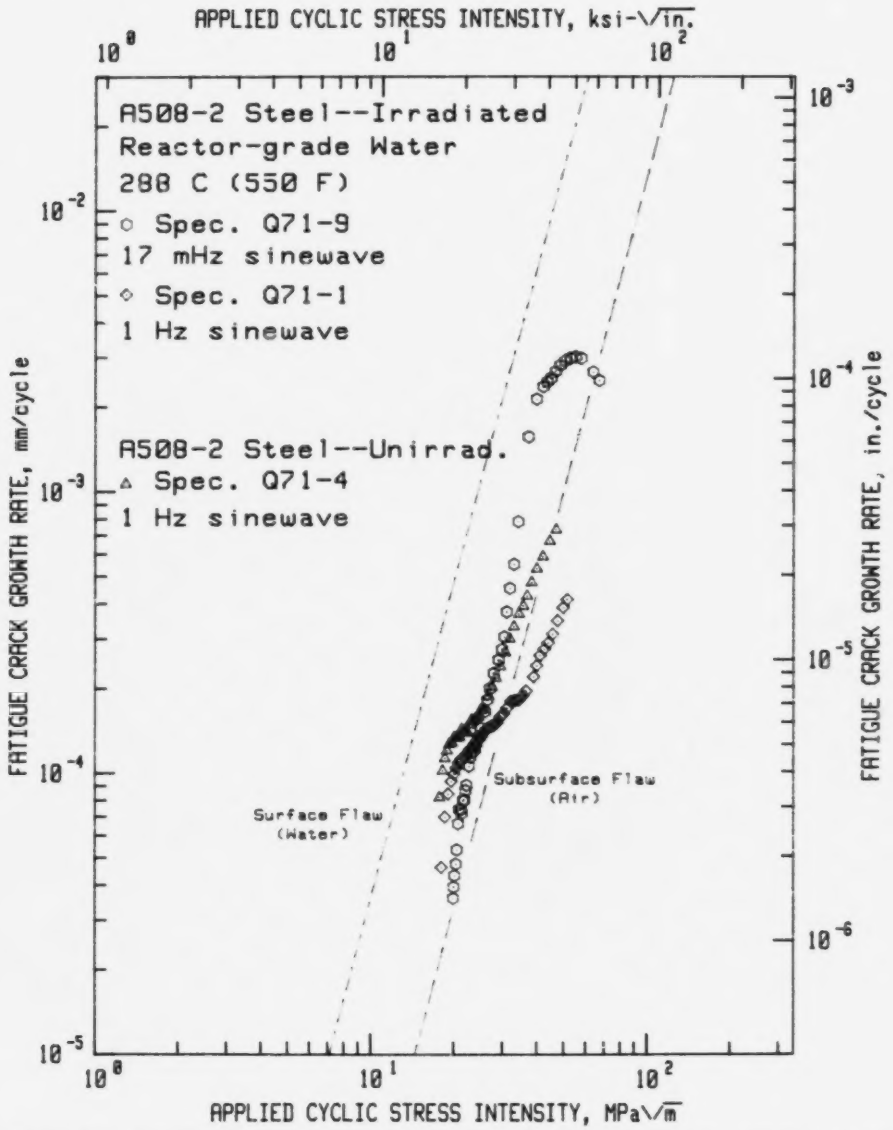

Fig. 11 - Fatigue crack growth rates vs applied cyclic stress intensity factor for irradiated and unirradiated, but reactor time-and temperature-conditioned, A508-2 steel. These results are very similar to those for A533-B shown in Figs. 9 and 10. In this case, the irradiated specimen tested at 1 Hz shows a slight, but measureable decrease in crack growth rates. Specimen Q71-1 was irradiated to a total fluence of 3.4×10^{19} n/cm^2 >1 MeV, Q71-9 to a total fluence of 4.5×10^{19} n/cm^2 >1 MeV.

carried out to a longer final crack length, and hence higher ΔK value than L83-6, the onset and extent of Region II growth behavior is more clearly described in this case. Note that the increase in growth rates between the 1 Hz and 17 mHz results is about a factor of twenty, while the increase in cyclic period is about sixty. The relationship is not, therefore, one-to-one, and in fact, if irradiation has little or no effect, we can expect, on the basis of unirradiated results [16,17] that the 17 mHz waveform affords a saturation or maximization of the environmental effect, for PWR environments. Thus, the 17 mHz results of Figs. 9 and 11 represent the probable upper limits of fatigue crack growth for the R = 0.2 constant-load-amplitude condition. The comparison of 1 Hz test results for irradiated, and unirradiated but time-and-temperature-conditioned specimens, also shown in Fig. 11 indicates that the irradiated results are somewhat lower than the unirradiated results, although the difference is not clearly greater than the commonly accepted scatter band (a factor of about two) for similar, intralaboratory fatigue crack growth rate tests.

As indicated in the section on unirradiated results, the code V82 forging has demonstrated an enhanced susceptibility to corrosion fatigue crack growth. Fortunately, as shown in Fig. 12, testing of an irradiated sample of the code V82 material produced crack growth rates nearly identical to the growth rates of an unirradiated specimen, indicating that irradiation damage did not further aggravate an already susceptible material. The V82-1 results are from 2T-CT specimen, and mark the completion of the first test with an irradiated specimen of this size.

The overall result derived from this study, that irradiation does not enhance crack growth rates at low load ratio, for simulated nuclear coolant environment, is parallel to the earlier results for tests in high and low temperature air environments [18]. In those instances of irradiated specimen results for which the growth rates are depressed (A508, code Q71, 1 Hz tests), this may be due to the increased yield strength of the irradiated specimen. In those cases for which the irradiated results are slightly higher than for comparable tests of similar materials (17 mHz tests-all cases), the increase may be due to a synergistic effect of the environmental influence on the radiation damaged steel, however, the variability is well within a scatter band defined by previous growth rate evaluations for these materials. In the case of the A508-2 forging, code V82, which seems to be slightly more environmentally susceptible than the code Q71 material, irradiation did not provide any further detrimental effects. It is important to note that for the specific sets of conditions studied (1 Hz and 17 mHz sinusoidal waveforms, R = 0.2, PWR conditions) none of the present results exceed the existing ASME default lines for aqueous environment fatigue crack growth.

c. Piping Test Matrix

Results from a test of A106 Grade C piping steel are shown in Fig. 13. These results are somewhat lower in growth rates than would normally be expected of an R = 0.2, 17 mHz sinusoidal waveform test of A508-2 or A533B steels. Testing of A106 Grade C steel at 288°C with an R = 0.7, 60 sec ramp/reset waveform continues, with very low growth rates being realized (See Table 3).

d. Variable Amplitude Tests

During this quarter a four-specimen daisy chain of stainless and ferritic piping steels was loaded in an autoclave and precracked in the environment. Unfortunately, a system malfunction resulted in a massive overload of the specimens, and the test assembly has been dismantled. Replacement specimens are being machined, and variable amplitude testing will resume at the next opportunity.

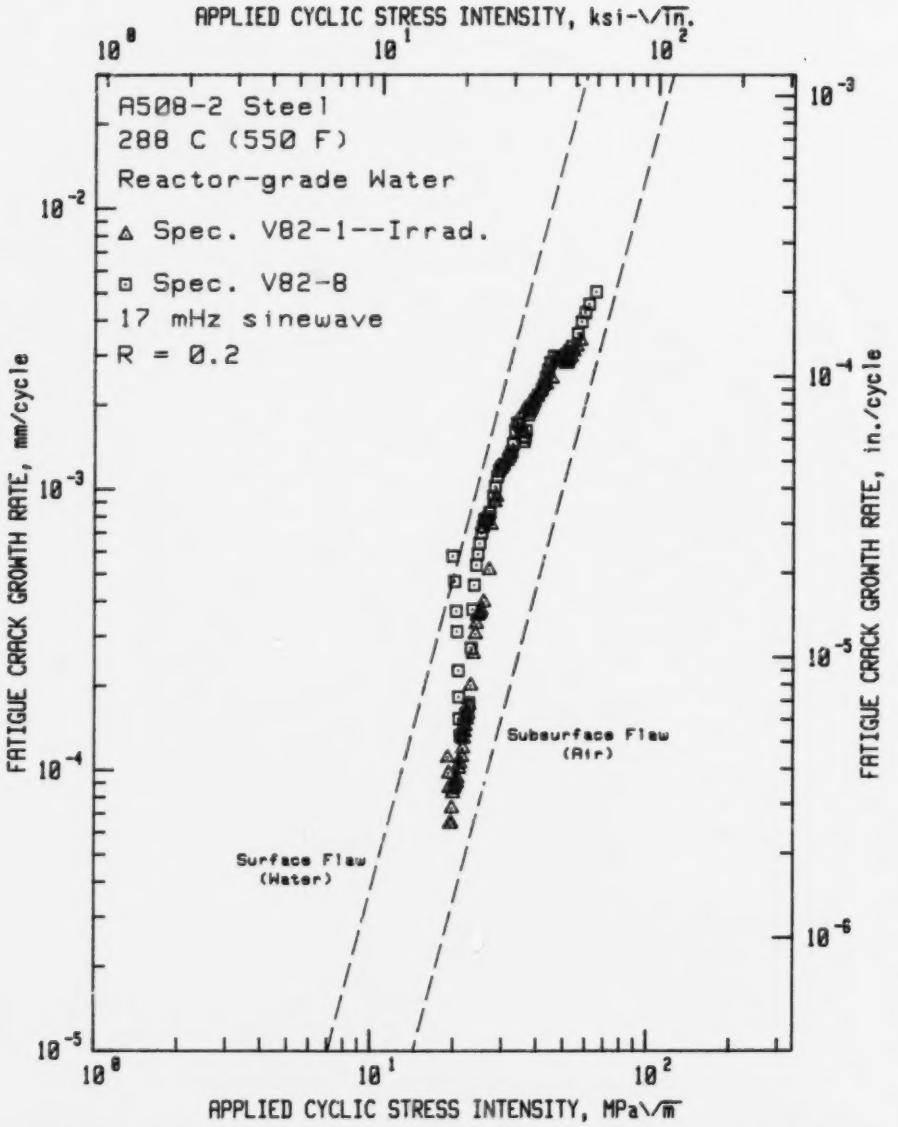

Fig. 12 - Fatigue crack growth rates vs applied cyclic stress intensity factor fcr irradiated and unirradiated, as received A508-2 steel in high-temperature, pressurized reactor-grade water. There is no observable effect of irradiation from these initial data. Specimen V82-1 was irradiated to a total fluence of 2.46×10^{19} n/cm^2 >1 MeV.

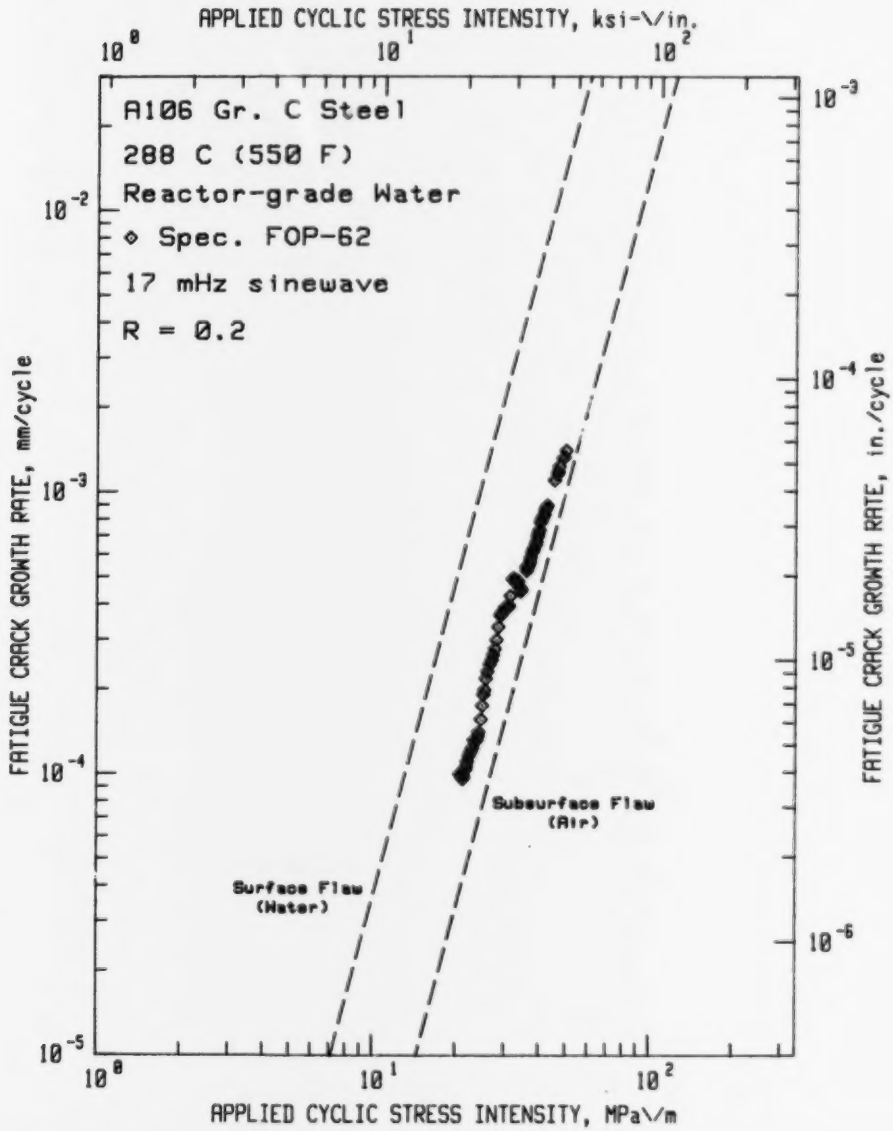

Fig. 13 - Fatigue crack growth rates vs applied cyclic stress intensity factor for A106 Grade C piping steel in high-temperature pressurized, reactor-grade water. These results are slightly lower than results for comparable tests on A508-2 or A533-B steels.

e. Supporting Tests and Extended Analysis of Data

(1) Three-Region Crack Growth Rate Behavior

During the initial phases of this research involving high-temperature, pressurized water environments, when test systems were being implemented and improved, and outages and other failures were frequent, common test practice was to choose an initial value of applied cyclic stress intensity (ΔK) such that relatively easily measureable crack extensions would occur over rather short times. Typically, for R = 0.2 and waveforms of about 60 sec periods, a ΔK value of 25 MPa $\sqrt{m}$ was selected. While the results of this research produced the desired amount of scoping data on the various materials [19], and enabled an understanding of temperature and waveform effects [16,17], the measurement of fatigue crack growth rates for lower stress intensity factor ranges (10-25 MPa $\sqrt{m}$ for R = 0.2) has not been adequately carried out. Now that the reliability of test and data acquisition systems has substantially improved, recent research has extended our understanding of fatigue crack growth rates into the lower ΔK ranges.

On the basis of these recent tests, it is becoming evident that fatigue crack growth rates for these reactor pressure vessel materials, at least for sinusoidal waveforms and low load ratios, follow the conventional three-region behavior which has been amply discussed in the classical presentations of stress-corrosion cracking [20] and corrosion-fatigue crack growth [21]. This is shown schematically in Fig. 14, which has been adapted, in a simplified way, to these results. The exact onset, in terms of ΔK, of the transition from Region I to Region II behavior is generally a function of the material and the environment. The level of Region II, in terms of crack growth rate, is primarily a function of test frequency, all other things being equal. The reader should note that Region I growth behavior should not be construed as an indication of "threshold," or lower limit behavior of these fatigue crack growth rates. The location of Region I for these data sets is simply a function of the initial value of ΔK chosen for these tests; true threshold studies on these materials have only been conducted for air environnments, with the results detailed in Ref. 21. The onset of Region II, the value of the growth rates throughout Region II, and the transition of Region II into Region III are established by the test frequency.

In illustration of this conclusion, fatigue crack growth rates for A508-2 steel are shown in Fig. 15, together with the trend lines shown in the previous figure. At the present time, this data describes the limits of the research completed on the extension of data into the lower ΔK regime. The drafting of the trend line for the air environment was based on work performed at Westinghouse Laboratories, in the early 1970's [21,22]. The data points which are shown are all from NRL research efforts; some of these data sets have been published earlier [23,16]. While this set of trend lines adequately describes the behavior of this material, there remain some aspects of this description for which additional research would be helpful. The exact position of the trend lines for lower values of ΔK, especially for longer period waveforms, is not well established. At the NRL, efforts are now underway to measure fatigue crack growth rates for 17 mHz (or comparable frequency) waveforms on tests for which the initial stress intensity factor was about 15 MPa$\sqrt{m}$. Similar efforts, in constant ΔK tests, with ΔK = 16.5 MPa$\sqrt{m}$, are underway at Babcock and Wilcox Research Laboratories, Alliance, Ohio. The data resulting from the above two efforts should assist in a more complete definition of the actual trends.

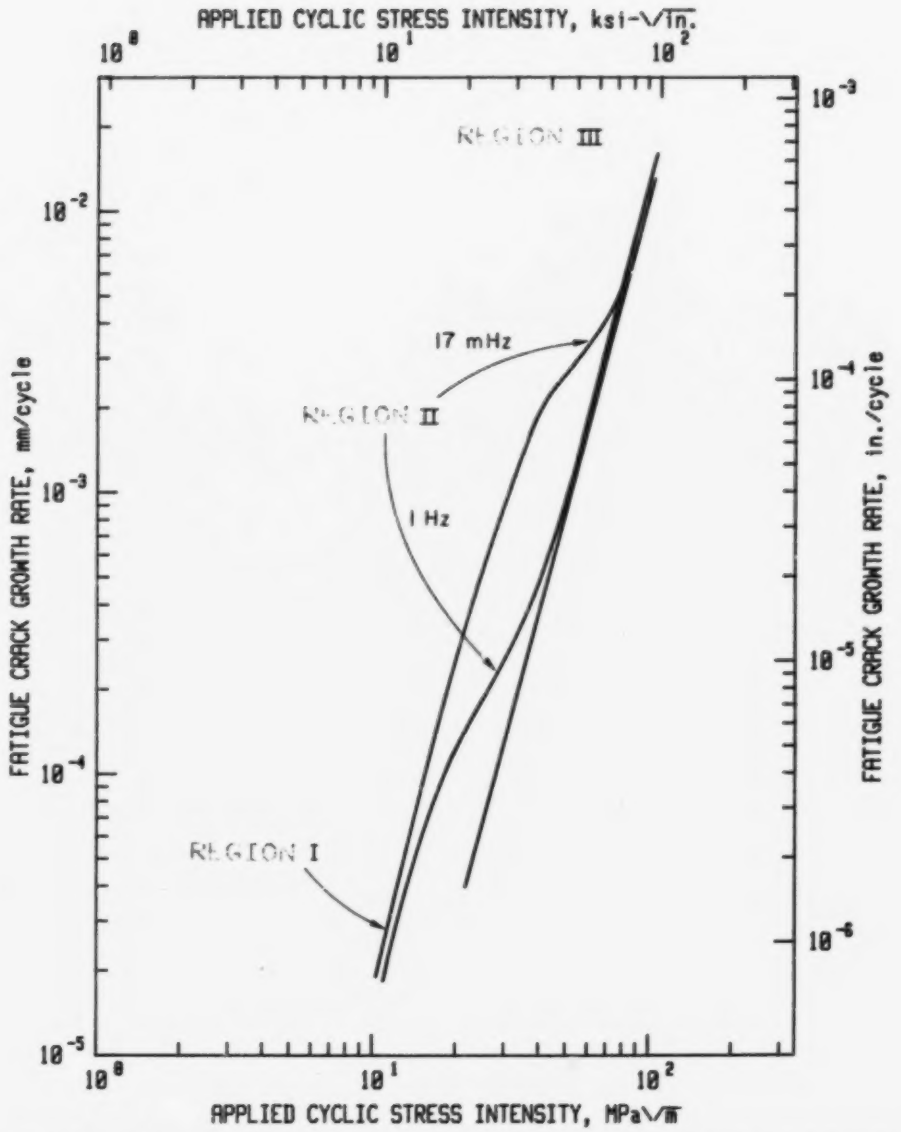

Fig. 14 - Trends of fatigue crack growth rates vs applied cyclic stress intensity factor for A508-2 forging. Region I represents the start-up regime, Region II the environmentally assisted growth regime, and Region III the mechanically-driven fatigue crack growth regime [21].

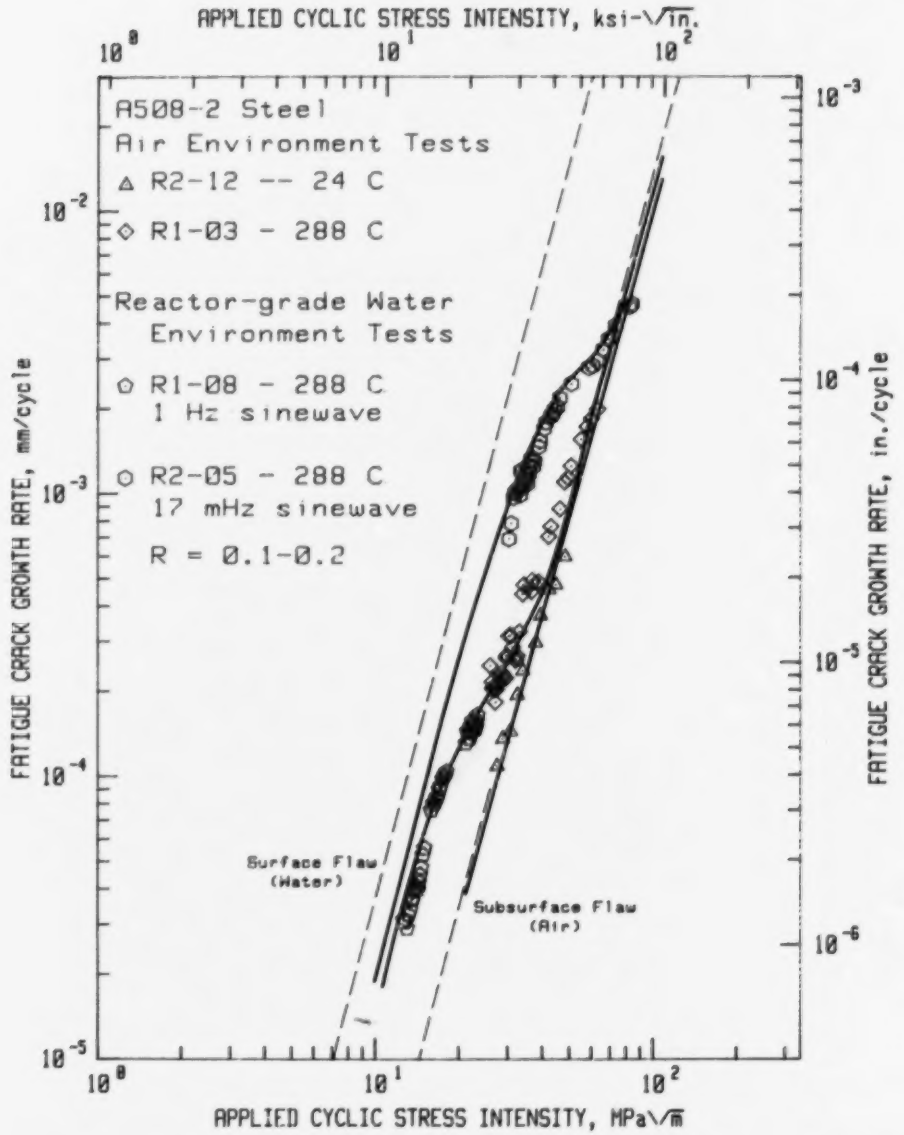

Fig. 15 - Fatigue crack growth rates vs applied cyclic stress intensity factor for A508-2 forging steel-code R, superposed on the trend lines of Fig. 14.

(2) Start-Up Transient Investigation

Ordinarily, fatigue crack growth rates (da/dN), whether environmentally assisted or not, increase monotonically with increasing applied cyclic stress intensity, ΔK. When plotted on logarithmic axes, this increase is not completely linear, which would imply a power law equation relating da/dN and ΔK. Instead the data defines a sigmoidal shape. As described previously in this section, the exact shape and position of the sigmoid is chiefly dependent on material, environment, frequency and waveform. However, many tests of RPV steels in high-temperature, pressurized water environment have produced FCGR which vary randomly, or monotonically decrease with increasing ΔK. This decrease occurs often at the beginning of a test (see Fig 8b and Figs. 4a, 43, 46, 53, 57, Ref. 19), but a few examples have been published for which the decrease was general throughout the test, (Figs. 30, 59, 60, Ref. 19).

Several explanations have been advanced in efforts to interpret this phenomenon. Most propose, in various ways, that the environment at the crack-tip is in a transient rather than a steady state, and that these transients are naturally occurring at test start-up, but may also be caused by changes in frequency or waveform, test interruptions, or other irregularities in test practice. In an effort to more accurately identify the causes and effects of these FCGR reversals, a change in fatigue test start-up procedure has been initiated. Once a specimen has been installed, the autoclave is sealed and the bulk environment is permitted to stabilize at a dissolved oxygen level of <1 ppb. Then the specimen is cycled with a 1 Hz sinusoidal waveform, using the test loads, such that the crack is extended for a distance of several millimeters. Additionally, the test loads are chosen such that the 1 Hz cycling, or pre-test, covers a ΔK range beginning with a value lower than that desired for the actual test, and the crack is allowed to extend until that desired ΔK is realized. Then the waveform is immediately converted to the shape and frequency which have been chosen for that particular test. The crack growth rates are carefully measured during the 1 Hz pre-test, as well as the actual test. The philosophy which underlies this practice stems from the belief that the crack tip environment must stabilize under the influence of the mechanical action of fatigue before the reliably monotonic increase in FCGR can be expected. The crack extension occuring during the pre-test creates, in theory, an opportunity for this steady-state behavior to develop.

In practice, the results are mixed, ranging from the best data which may be expected, i.e., a smooth transition between the pre-test and actual test, and monotonically increasing behavior in both regimes, to more difficult to understand data, exhibiting wide variations and reversals. Some results are presented in Figs. 16, 17 and 18. These are graphs of crack growth rate as a function of crack length. Presenting the data in this somewhat unorthodox format is more meaningful for this type of study since it shows how much crack growth is necessary for the various perturbations to smooth out. The accuracy of the graphs is further enhanced by the acquisition of a large number of data points, a practice made possible through use of a fully automated, computerized data acquisition system.

Figure 16 shows results from the testing of specimen Q71-9. This 1T-CT specimen had been pre-cracked in air, and then irradiated. The autoclave test involved $\sim$3 mm of crack growth with a 1 Hz, sinusoidal waveform, followed immediately (within minutes) by a conversion to a 17 mHz sinusoidal waveform. Examination of the 1 Hz portion of the data shows that after about 1 mm of crack growth, the growth rate increased sharply until Region II growth was begun. The growth rate then continued on a significantly lower slope for about 1 mm, at which time the conversion to 17 mHz sinusoidal waveform was applied. That the change in slope denoting entry into Region

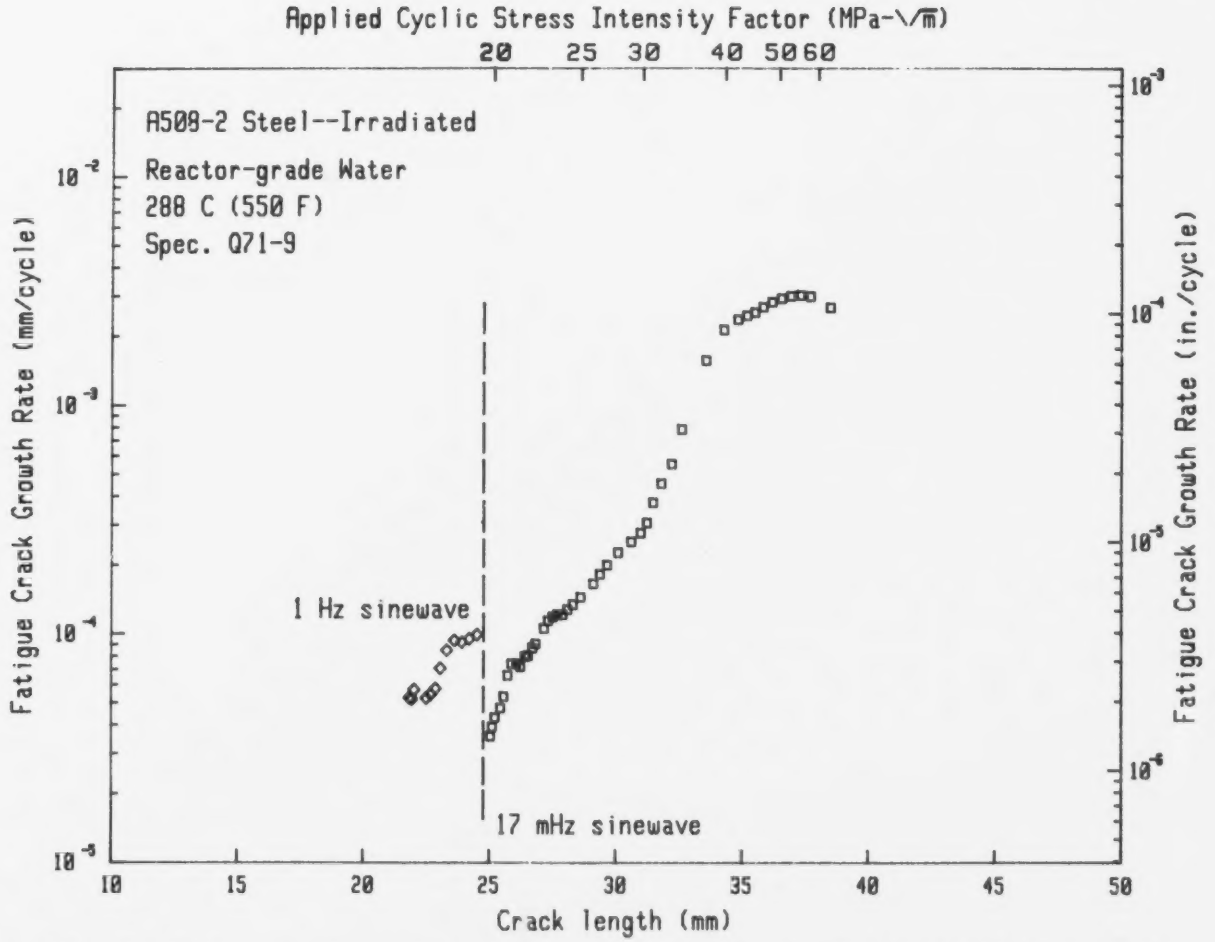
Applied Cyclic Stress Intensity Factor (MPa-√m)
20 25 30 40 50 60
A508-2 Steel--Irradiated
Reactor-grade Water
288 C (550 F)
Spec. Q71-9
1 Hz sinewave
17 mHz sinewave
Fatigue Crack Growth Rate (mm/cycle)
Fatigue Crack Growth Rate (in./cycle)
Crack length (mm)
10 15 20 25 30 35 40 45 50

Fig. 16 - Fatigue crack growth rate vs crack length for irradiated A508-2 steel. This 1T-CT specimen was tested in two phases: 1 Hz sinusoidal waveform for about 3 mm of crack extension, followed by a 17 mHz sinusoidal waveform for the main part of the test. The initial crack growth rate for the 17 mHz test fails to reside as high as that at the end of the 1 Hz portion of the test.

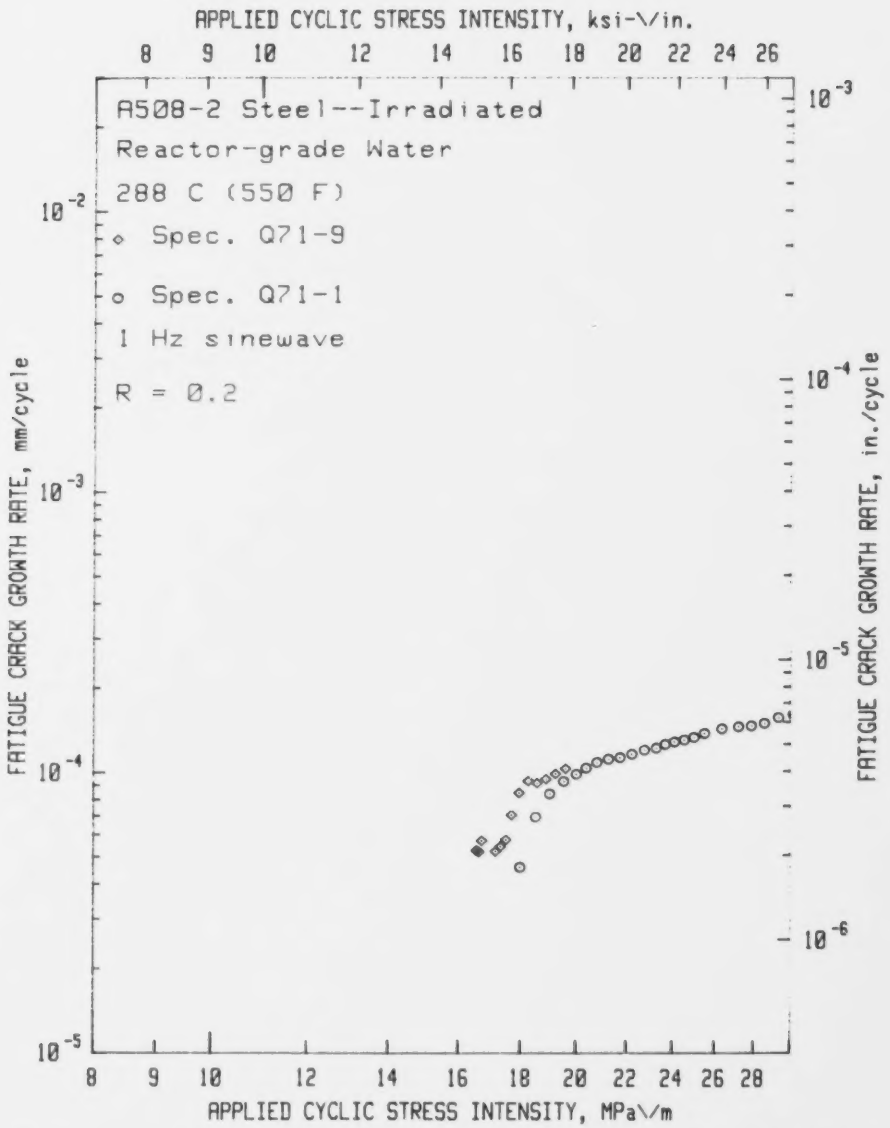

Fig. 17 - Fatigue crack growth rate vs applied cyclic stress intensity for irradiated A508-2 steel tested with a 1 Hz sinusoidal waveform. This is plotted on an expanded abcissa so that the densely packed data can be better delineated. This plot indicated that Region II behavior had been attained by specimen Q71-9 prior to conversion to a 17 mHz test frequency.

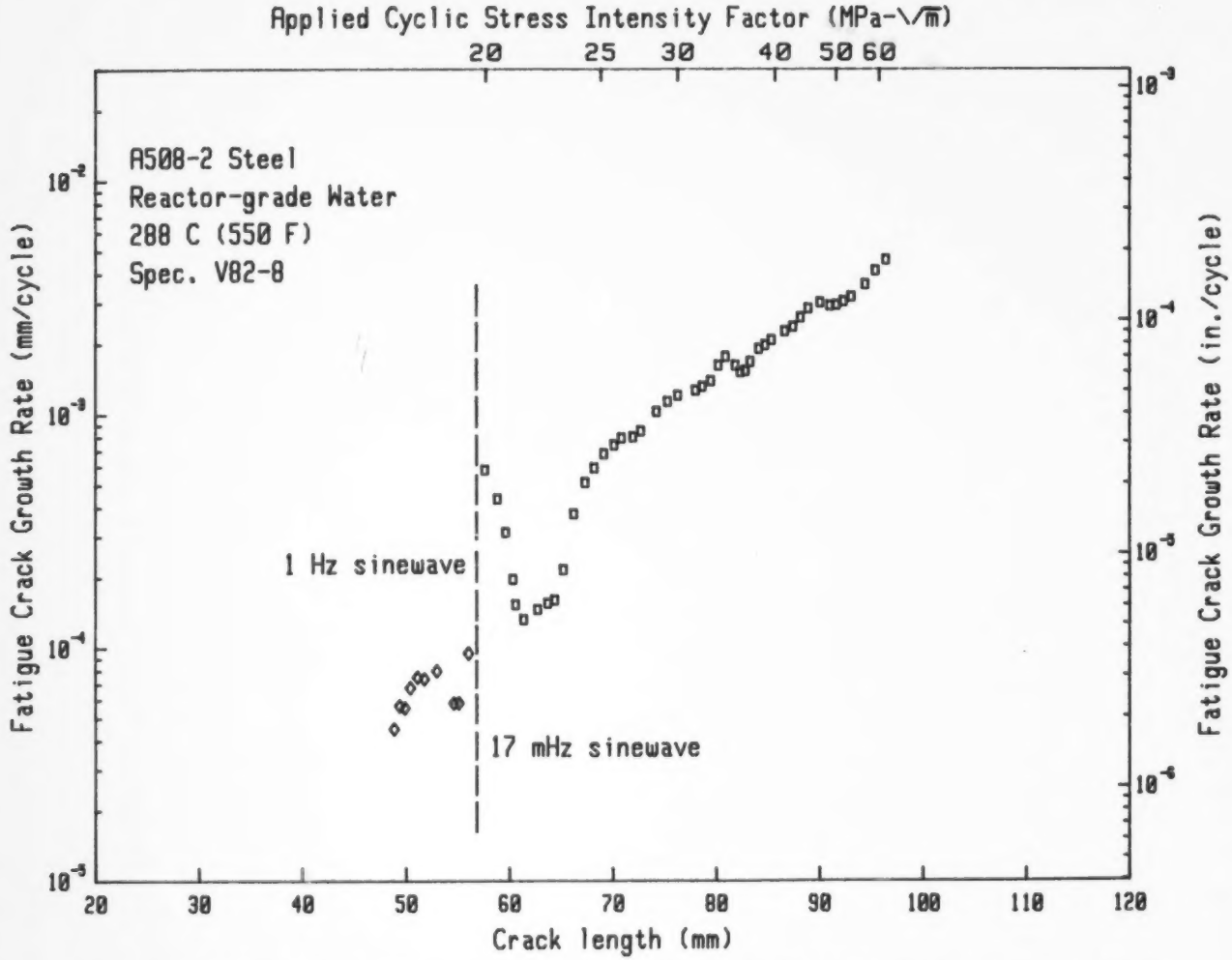
Applied Cyclic Stress Intensity Factor (MPa-√m)
20 25 30 40 50 60
A508-2 Steel
Reactor-grade Water
288 C (550 F)
Spec. V82-8
1 Hz sinewave
17 mHz sinewave
Fatigue Crack Growth Rate (mm/cycle)
Fatigue Crack Growth Rate (in./cycle)
Crack length (mm)
20 30 40 50 60 70 80 90 100 110 120

Fig. 18 - Fatigue crack growth rate vs crack length for A508-2 steel. Similar to the data shown in Fig. 16, this specimen was tested with a 1 Hz sinusoidal waveform for about 8 mm of crack extension followed by testing with a 17 mHz sinusoidal waveform. In this case, an initially high crack growth rate for the 17 mHz test is followed by a significant decrease and an equally rapid increase.

II controlled growth is not random can be seen from comparison of these 1 Hz results with those of specimen Q71-1 (Fig. 17). The latter is an irradiated specimen of the same material also tested at 1 Hz but over the entire available ΔK range. The data from the 1 Hz portion of the Q71-9 test trends right into that from Q71-1. The point here is that the steady-state potentiokinetic relationship which results in Region II behavior had been established before the waveform conversion. Yet, just after the conversion, the growth rates dropped by a factor of about three, in spite of the longer cyclic period, which should have led, if anywhere, to even higher growth rates. Furthermore, about 8 mm of crack extension occured before Region II behavior was initially attained for the 17 mHz waveform.

Data from other specimens shows different trends, helping further to confuse the explanation of this phenomenon. As an example of a behavior somewhat inverse to that of Q71-9, the data from specimen V82-8 is shown in Fig. 18. This is a 2T-WOL specimen of unirradiated A508-2 steel which had been precracked in air. The autoclave test involved about 8 mm of crack growth with a 1 Hz sinusoidal waveform, followed immediately by a conversion to a 17 mHz sinusoidal waveform. In this case, instead of a decrease in crack growth rate upon conversion of waveform (as in specimen Q71-9) there is an increase by a factor of about 8. Over the next 5.5 mm of growth, this rate decreased, then increased once more to the Region II levels typical of this waveform.

Observation of the crack growth behavior following a change in test frequency is just one of several transient effects which are being currently investigated. Effects of test interrruptions, minor overloads, and environmental irregularities, such as changes in dissolved oxygen content are also being studied. However, the test time required to accurately perform such evaluation is quite extensive, especially for the longer period waveforms. Also, the enthusiasm with which this is pursued should reflect the engineering necessity for such data, since the total number of 17 mHz frequency stress cycles in a typical reactor lifetime is expected to be relatively small.

(3) Crack Growth Rate Dependence on Dissolved Oxygen Content

The above discussion not withstanding, the research on fatigue crack growth rates has provided some firm conclusions about the overall trends or dependencies of the data on temperature, waveform and load ratio. However, the variability in these experimentally determined values can be seen in a recent review [19], and in the results of a round robin test series (to be published in the future) conducted by the ICCGR) Group. From the round robin results particularly, it is apparent that FCGR tests, conducted under nominally identical conditions, can yield widely varying results, and these disparities have been, and are, a subject of some concern. These same results may, however, shed some light on a possible source for this variability. Briefly, participants were asked to run two FCGR tests, at 288°C, in deionized water, with test frequencies of 17 mHz and 1 Hz respectively. The 1 Hz test results reside on, or very near, the ASME Section XI air default line, while 17 mHz results are rather evenly scattered throughout the band defined by the ASME air and water default lines. To the present time, only the NRL [18] and Westinghouse [24] results have been formally released.

That the 1 Hz results reside on the ASME air line, and that they are reproducible, with relatively little scatter, by the various laboratories, is not surprising, since the frequency is high enough that environmental effects are circumvented, and the test is short enough ($\sim$9 hr test time) that major interruptions due to equipment malfunctions have a low probability. Essentially, since the test began at a ΔK value of 27.5

MPa m, participants were measuring crack growth rates for Region III behavior of this steel.

On the other hand, the 17 mHz test frquency is low enough that the bulk of the data, from these tests, which also started at an initial ΔK value of 27.5 MPa $\sqrt{m}$, should describe Region II, or the environmentally assisted regime of the FCGR trend lines described earlier. As a consequence, these data sets exhibit a dependence on the characteristics of the environment, and indirectly, a dependence on test practice, where it affected the environment or, more subtly, the environmental equilibrium at the crack tip. In particular, the dissolved oxygen content of the environment appears to have a strong influence on the results.

The laboratories which participated in the round robin tests can be partitioned into three basic categories:

(a) Those who operate continuously circulating, closed, relatively small volume autoclaves, with a proven capability to maintain less than a 1 or 2 ppb dissolved oxygen content. These laboratories reported rather high crack growth rates (near the ASME water line).

(b) Those who operate large volume circulating, or once through flowing water systems, or those with newer systems which do not yet have the integrity to maintain ultra-low dissolved oxygen levels. Although approximate, it seems reasonable, in the opinion of the authors, to assume that these autoclaves are operated at a 10 to 50 ppb dissolved oxygen level. In many cases, the laboratories in this category have not implemented accurate dissolved oxygen analysis procedures, and the above operating range can be neither verified or denied. As a group, these laboratories reported rather low crack rates, compared to those laboratories in category (a) or (c).

(c) Those who attempt to simulate boiling water reactor coolant environments, and who deliberately maintain high (200 ppb or greater) levels of dissolved oxygen. Also included in this group is a laboratory whose operating procedures involved opening the autoclave several times during the test, to check on progress of the fatigue crack. This procedure probably resulted in an unavoidable oxygenation of the water in the system. As a group, the results from these laboratories reside near, or above the ASME water default line.

The following discussion proposes a connection between the dissolved oxygen content of the test systems and the FCGR results which were realized. The basis for the development of this explanation can be found in the work of Indig [25]. For a temperature of 274°C, Indig described an electropotential diagram for a SA333 steel-oxygen system in which low concentrations of dissolved oxygen (DO_2) result in a low level of corrosion potential, high DO_2 concentrations result in a high potential, and intermediate levels (8 to 20 ppb) define a very sharp transition between these two regimes. Thus for near-zero levels of dissolved oxygen, dissolution-type reactions are virtually insignificant, but as the oxygen level increases, dissolution activity becomes more pronounced, essentially saturating for (in these cases) values of dissolved oxygen greater than about 20 ppb. In a related piece of applicable evidence, Parkins [26] has described an oxide filming process which may take place in metal-water systems containing very low concentrations of dissolved oxygen. To describe the effect of these electrochemical phenomena on fatigue crack growth rates, the schematic shown in Fig. 19 can be drawn. For tests in which all variables (temperature, materials, waveform, ΔK, etc) are equal, except for DO_2 levels, fatigue crack growth rates are found to be high, for very low (near-zero) DO_2 levels (Regime A) decreasing to

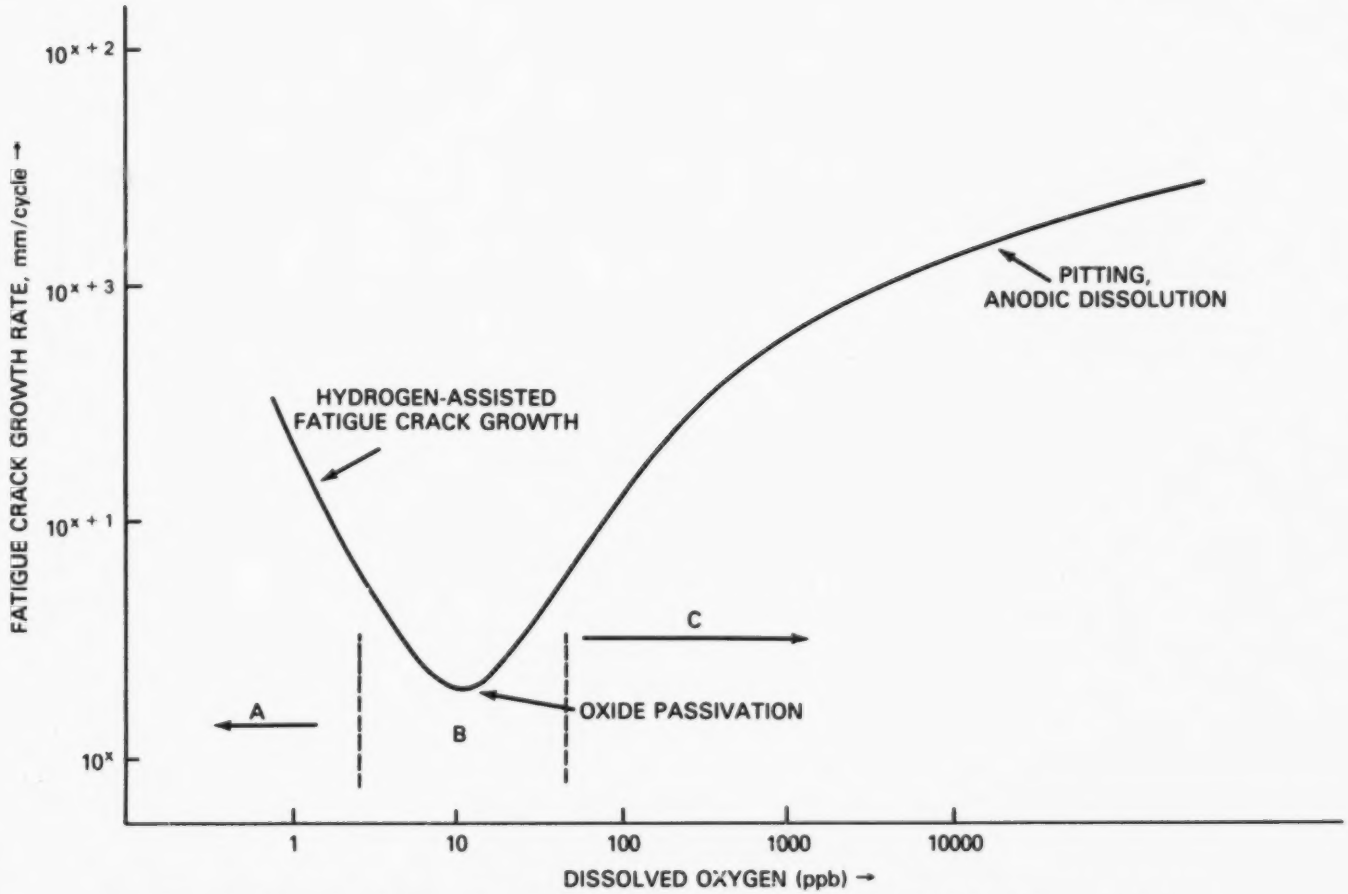

Fig. 19 - Fatigue crack growth rates anticipated for a hypothetical high-temperature, pressurized, reactor-grade water test in which all external variables are held constant except dissolved oxygen content.

substantially lower rates for intermediate DO_2 levels (Regime B) then trending high again for rather large contrations of DO_2 (Regime C).

The mechanistic explanation of this combines the attributes of a hydrogen-assisted crack growth model [16], the filming and passivation described by authors such as Indig and Parkins, and the anodic dissolution model, recently reviewed by Ford, [27] which is often invoked by the researchers involved in BWR cracking problems. The following description is aided by the curve shown in Fig. 19. This curve is intended to represent the fatigue crack growth rates which might be expected in a (hypothetical) test in which all external variables (ΔK, waveform, temperature, etc) have been fixed, and only dissolved oxygen content allowed to vary. For this reason, the ordinate axis is graded in arbitrary powers of ten.

For the very lowest DO_2 levels, there is not enough oxygen to cause any significant effect, either detrimental or constructive, and the uninhibited take-up of hydrogen species resulting from hydrolysis of the environment at the crack tip proceeds easily. This results in a significant hydrogen-assisted fatigue crack growth component, and as a consequence, the fatigue crack growth rates are fairly high, as indicated by region A in Fig. 19. For small, but somewhat significant amounts of oxygen (about 5 to 50 ppb), the filming processes discussed by Parkins [26] passivate the crack tip, without providing detrimental component to the cracking process. In fact, it seems likely that the passivating action inhibits the absorption and transport of the hydrogen into the metal matrix. Fatigue crack growth must then proceed without either a hydrogen assistance or oxygen dissolution component, and crack growth rates are depressed to essentially their lowest level. This is represented by region B in Fig. 19. As the oxygen content in our hypothetical experiment is increased, the oxygen attack at the crack tip transforms from the very passivating type of oxidation to a more aggressive reaction, involving pitting corrosion, which provides an easily measureable acceleration to the fatigue crack growth rates. It may also be possible that the morphology of the oxidation products which are formed at the crack tip [17] may also be porous enough that the hydrogen assistance mechanism, which had been successfully defeated for the mid-range DO_2 levels, might be reactivated at these higher levels, so that two detrimental mechanisms might be at work. The overall result is the high growth rates shown by region C of Fig. 19.

To connect the model suggested above to the earlier discussion of the laboratories involved in the ICCGR round robin tests, the reader should note the laboratories in category (a), with autoclaves featuring extremely low DO_2 contents, produced rather high growth rate results, with fractographic results [17] indicating a hydrogen asistance mechanism. Laboratories in category (b), featuring intermediate values of DO_2 content, produced low crack growth rates, suggesting a passivated crack tip, and category (c) laboratories produced the characteristically high crack growth rates expected of a low-frequency test in the high-DO_2, BWR-type environments which favor pitting and anodic dissolution mechanisms.

B. Corrosion Fatigue Crack Growth Behavior of Pressure Vessel Steels

W. H. Bamford* and L. J. Ceschini*

INTRODUCTION

The objective of this program is to characterize the fatigue crack growth rate properties of ferritic pressure vessel steels exposed to PWR primary coolant environments. Two environmental chambers are being used, and the tests presently underway are listed in Table 4. Three areas are being investigated - characterization of weld/heat affected zone materials, study of mechanisms and starting effects, and evaluation of static load cracking susceptibility.

TABLE 4 - Tests Underway as of June 1, 1980

Specimen (2T-CT)	Loading	R Ratio
D-2HAZ	17 mHz Sine Wave	0.7
R-22	17 mHz Sine Wave	0.7

During this reporting period testing was completed on the first three specimens of a new weld being studied under the program, made with Linde 0091 flux. Further studies have been made of the fracture surfaces of previously tested specimens, and some discussion will be included of environmental chemistry.

A potentially important trend is now appearing in the crack growth rate results. It appears that the susceptibility of these steels to environmental influence is related to the inclusion content, in particular the manganese sulfide inclusions. This trend will be discussed both in terms of observed behavior and possible mechanisms involved.

CRACK GROWTH BEHAVIOR OF WELDS AND HEAT-AFFECTED ZONES

This reporting period saw the completion of three specimens as part of the test matrix shown in Table 5. The specimens were all from a weld made with Linde 0091 flux, the third weld to be studied. Results of the individual specimens are shown in Figs. 20 through 22.

It is evident from these three figures that the crack growth rates do not show nearly as much environmental influence as earlier base metal results, represented by the upper scatterband lines in the figures. For example, a comparison of the results in Fig. 20 with results obtained on the two other welds studied thus far is provided in Figs. 23 and 24.

All the test results shown in Figs. 20 through 24 are for the same simulated PWR environment and for sinusoidal loadings at 17 mHz, or one cycle per minute. It is seen that the test and environmental conditions are comparable, with the only difference being the material themselves. Study of the material chemistries shows that there are significant differences in the sulfur content of the Linde 0091 weld as compared in the previous two welds tested, and this may help to explain the behavioral differences. The chemistry of each of the welds tested thus far is given in Table 6 [28,29], and the effects of such chemistry differences are discussed below.

* Westinghouse Electric Corp.

TABLE 5 - Test Specimens Weld and Heat-Affected Zones

Material	Test Conditions			
	R = 0.2		R = 0.7	
	One Cycle Per Minute	One Min-Ramp No Hold	One Cycle Per Minute	One Min-Ramp No Hold
Linde 124 Weld (2TWOL)	C-2 C-3	C-7 C-9	C-1 C-6	C-8 C-10
Linde 124 Weld HAZ (In A533-B Cl 1 Plate) (2TCT)		C-24-HAZ-1		C-23-HAZ-1
Linde 80 Weld (2TCT)	C-3-WLD C-6-WLD	C-1-WLD C-5-WLD[b]	C-4-WLD C-7-WLD	C-2-WLD
Linde 80 Weld HAZ (In A508 Cl 2 Forging) (2TCT)	C-3-HAZ	C-1-HAZ	C-4-HAZ	C-2-HAZ
Linde 0091 Weld (2TCT)	D-1-WLD[a] D-3-WLD[a]		D-2-WLD*	
Linde 0091 Weld HAZ (In A533-B Cl 1 Plate) (2TCT)	D-1-HAZ			

[a]Completed during this reporting period.

[b]30 sec ramp, no hold.

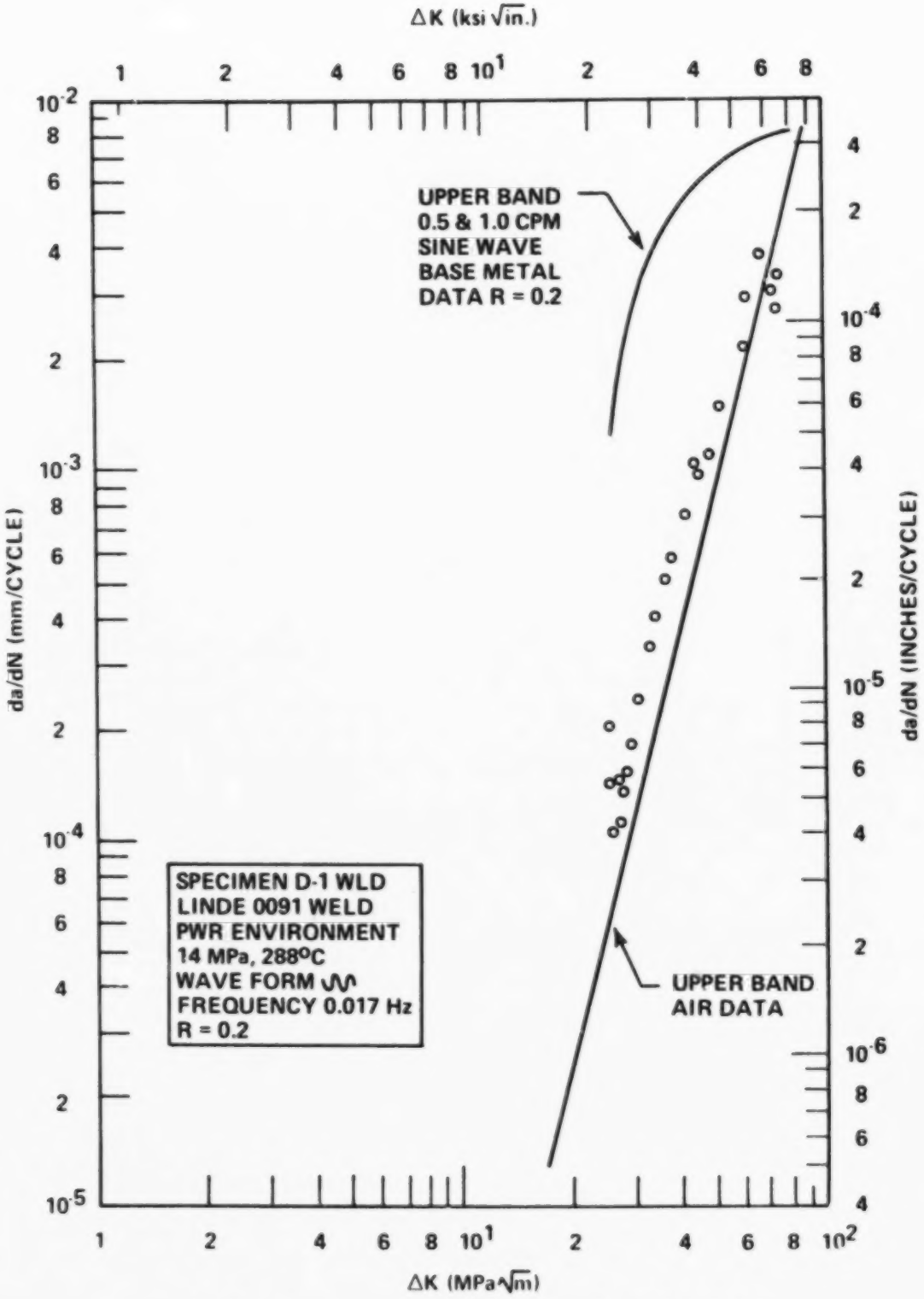

Fig. 20 - Crack growth results for specimen D-1 WLD.

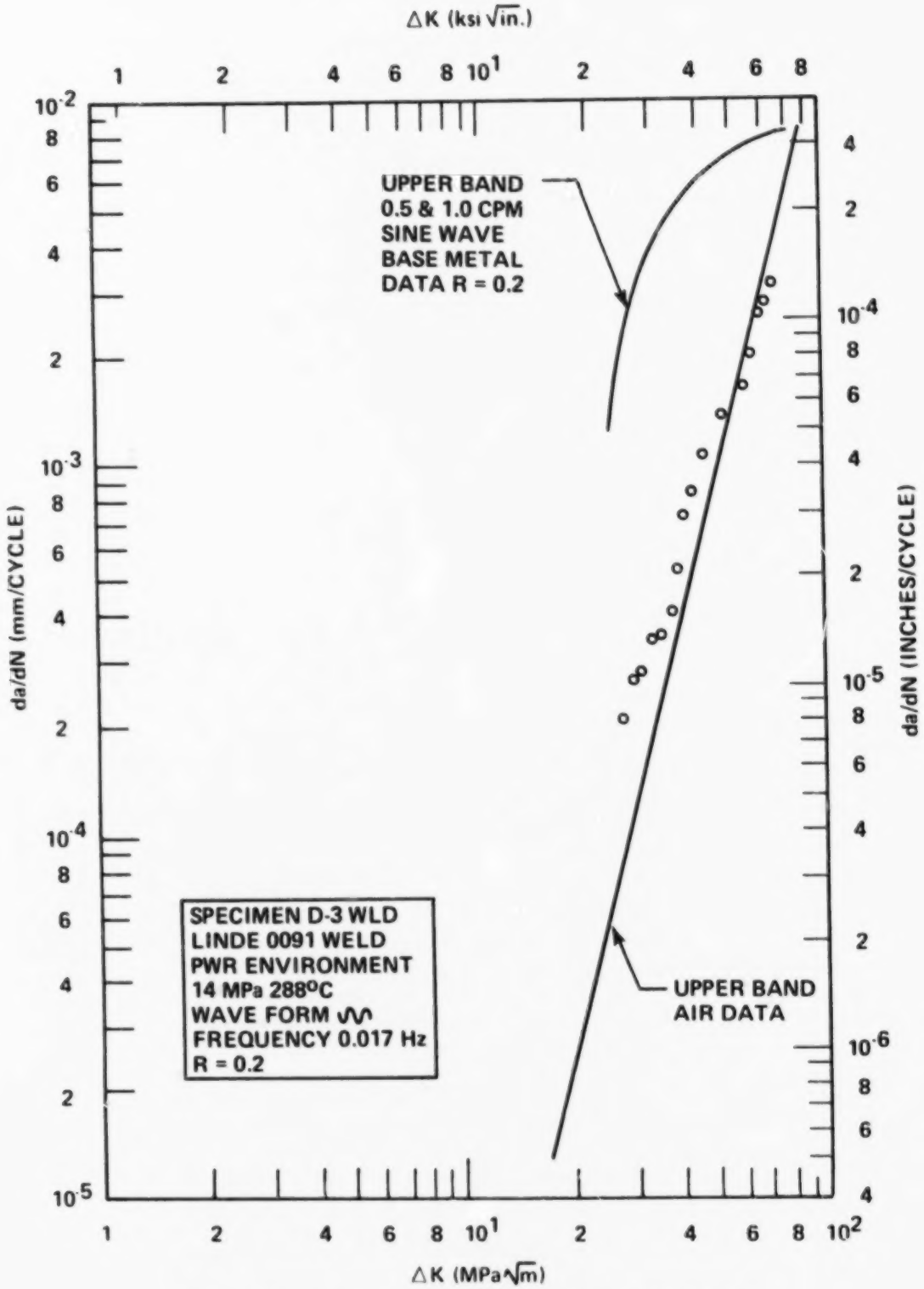

Fig. 21 - Crack growth results for specimen D-3 WLD.

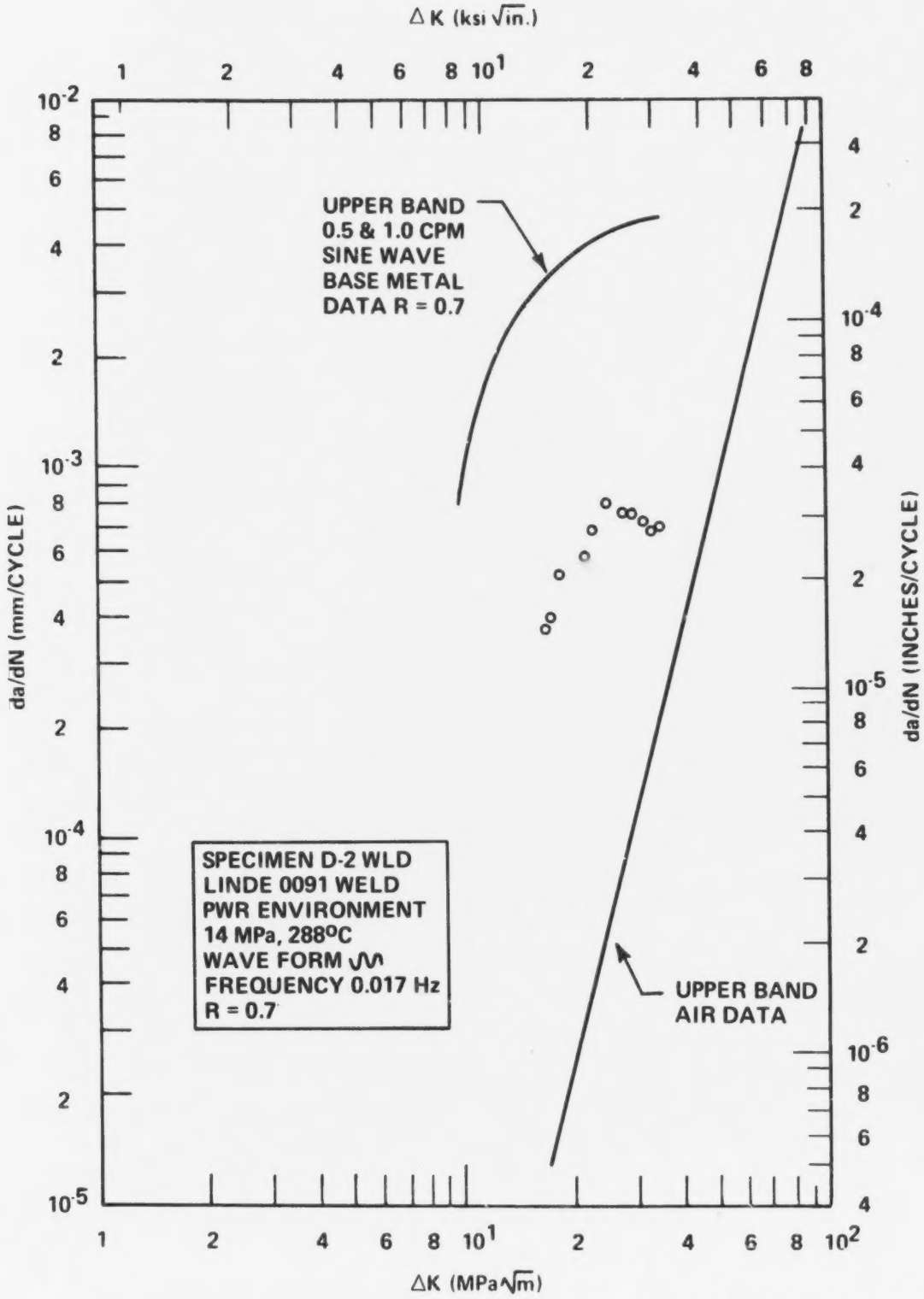

Fig. 22 - Crack growth results for specimen D-2 WLD.

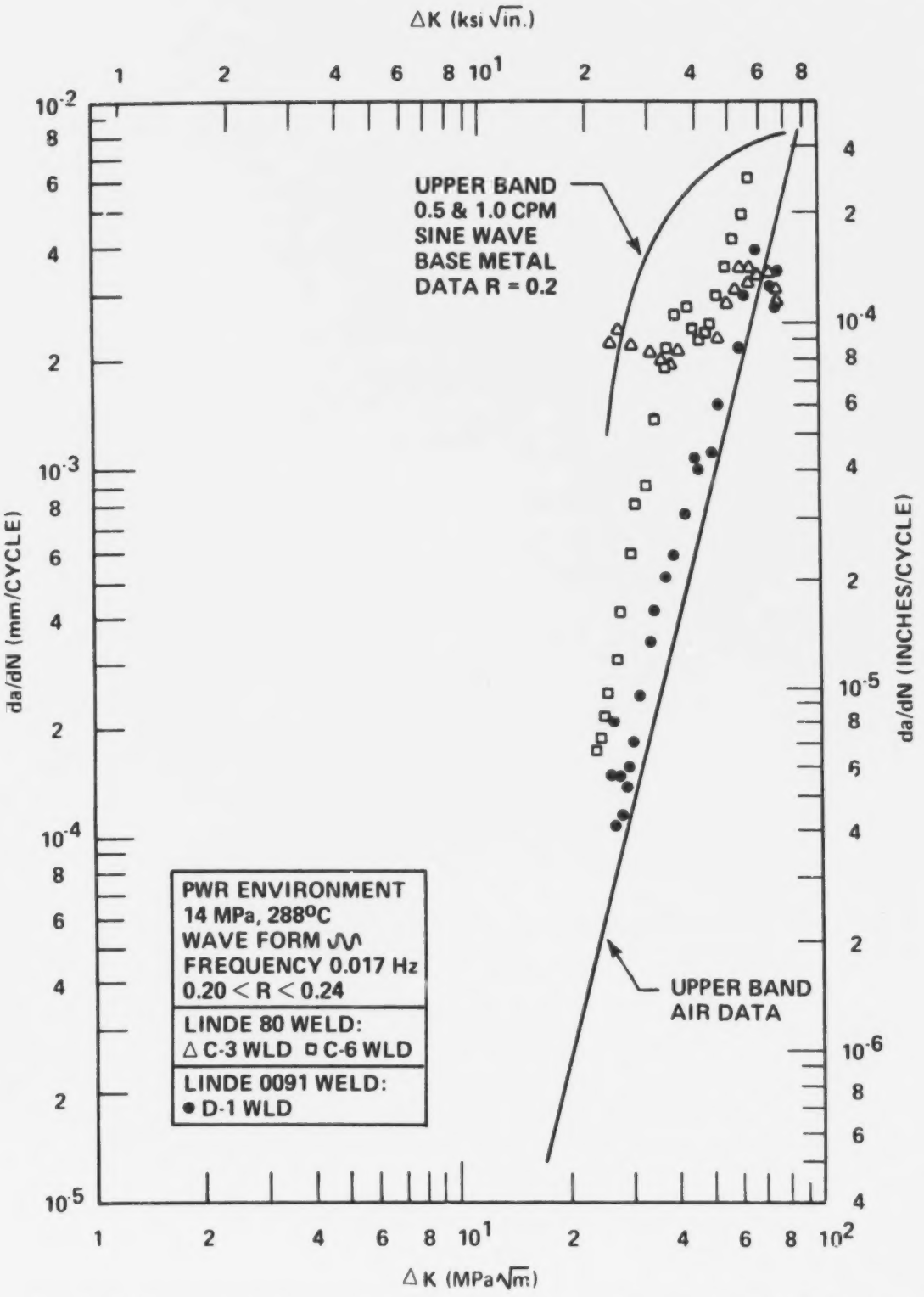
ΔK (ksi √in.)
1 2 4 6 8 10¹ 2 4 6 8
10⁻² 8 6 4 2 10⁻³ 8 6 4 2 10⁻⁴ 8 6 4 2 10⁻⁵
da/dN (mm/CYCLE)
4 2 10⁻⁴ 8 6 4 2 10⁻⁵ 8 6 4 2 10⁻⁶ 8 6 4
da/dN (INCHES/CYCLE)
UPPER BAND
0.5 & 1.0 CPM
SINE WAVE
BASE METAL
DATA R = 0.2
PWR ENVIRONMENT
14 MPa, 288°C
WAVE FORM √√
FREQUENCY 0.017 Hz
0.20 < R < 0.24
LINDE 80 WELD:
△ C-3 WLD ▫ C-6 WLD
LINDE 0091 WELD:
● D-1 WLD
UPPER BAND
AIR DATA
1 2 4 6 8 10¹ 2 4 6 8 10²
ΔK (MPa√m)

Fig. 23 - Comparison of crack growth results for Linde 0091 and Linde 80 welds.

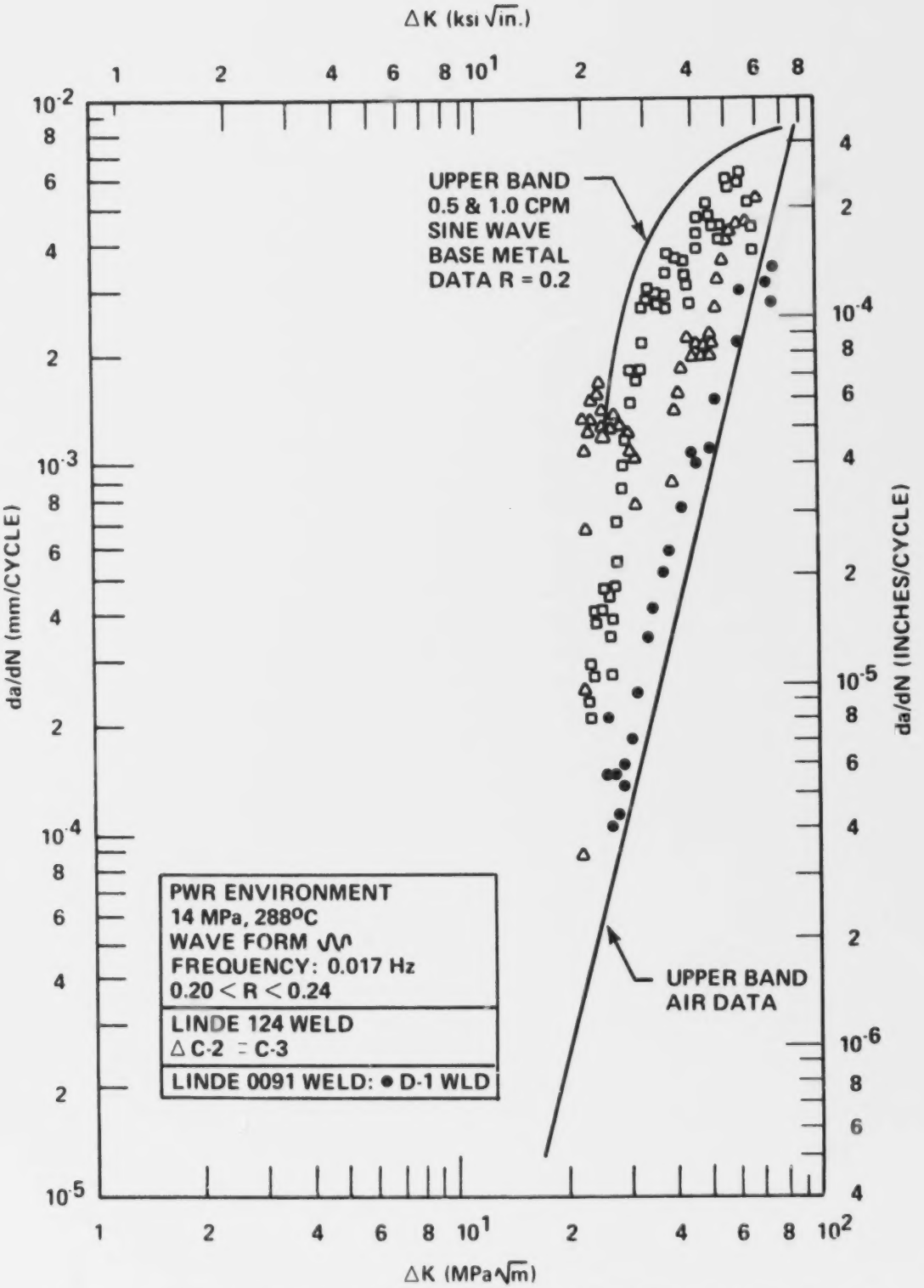

Fig. 24 - Comparison of crack growth results for Linde 0091 and Linde 124 welds.

TABLE 6 - Chemistry of Welds Studied to Date

(Vendor's Analysis)

MATERIAL	C	Mn	P	S	Si	Ni	Cr	Mo	Cu	V
Weld "C" (Linde 124)	.085	1.32	.013	.012	.48	.91	.14	.49	.05	.005
Weld "D-WLD" (Linde 0091)	.14	1.06	.012	.008	.20	-	-	.48	.15	-
Weld "C-WLD" (Linde 80)	.085	1.36	.019	.014	.42	.54	.06	.37	.18	-
ASTM Requirements [28]:										
A533-B Cl 1	.25	1.15-1.50	.035 max	.040 max	.15-.40	.40-.70	-	.45-.60	.10 max	.05 max
Beltline A533-B Cl 1	.25	1.15-1.50	.012 max	.015 max	.15-.40	.40-.70	-	.45-.60	.10 max	.05 max
A508 Cl 2	.27	.50-1.00	.025 max	.025 max	.15-.40	.50-1.00	.25 max	.45-.60	.10 max	.05 max
Beltline A508 Cl 2	.27	.50-1.00	.012 max	.015 max	.15-.40	.50-1.00	.25 max	.45-.60	.10 max	.05 max
ASME Requirements [29]: Submerged arc weld Type B4 (max)	.12	1.60	.012	.015	.080	-	1.75-2.25	.40-.65	.08	.05

EFFECTS OF CHEMISTRY AND PRODUCT FORM

The inclusion content of the welds studied appears to be influencing the amount of environmental acceleration obtained in corrosion fatigue crack growth rate tests. In particular, the manganese sulfide inclusions are measured by the sulfur content listed in the material chemistry. The sulfur level of 0.008 wt. percent in weld "D-WLD" is significantly below the levels for the two other welds tested.

The effect of inclusions on the fatigue crack growth and toughness of A533-B plate was recently studied by Wilson [30,31]. He showed that there can be important differences in the inclusion contents of these plates as a function of both steel making practice and sulfur content. Lowering the sulfur content has long been known to improve the upper shelf fracture toughness of these steels, but the effect on fatigue crack growth had not been studied. Wilson found that high inclusion content had a measurable effect on the crack growth rates, particularly important in crack propagation through the plate thickness. He also found that when the effect was greatest, the crack growth rate displayed a wavy effect on a logarithmic plot of crack growth rate versus range of stress intensity factor, adding to the scatter.

The effect of inclusions on environmental fatigue crack growth has not been studied systematically, but it seems that the possibility exists for a significant impact here. The water environment could react with manganese sulfide to form polythermic acid or hydrogen sulfide. Both of these compounds would act to lower the pH level of the water in the crack tip region. Even minute amounts can cause the corrosion potential to drop very quickly, enhancing a hydrogen mechanism, which is thought to be causing the environmental acceleration of crack growth [32]. Thus the effect of these inclusions on environmental enhancement of crack growth could be much more important than their effect on growth in air.

This effect has also been seen in crack growth rate test results as yet unpublished on a series of steels tested in France [33]. It also is consistent with an observation made by Cullen, et. al, in the previous progress report of this series [14]. It was reported there that a specimen from material V82 was "considerably more susceptible to fatigue crack growth in the high temperature, pressurized water reactor environment." The sulfur content of this forging was 0.012, about 50 percent higher than other forging materials tested there, which showed much lower growth rates.

Some caution should be exercised here in reaching the conclusion that this effect is fully verified. Although the observations here do seem consistent with several sets of available data, it remains to be demonstrated that the manganese sulfide inclusions will be able to create a crack tip environment active enough to promote hydrogen uptake. Some pilot tests are planned to study this subject during the next report period.

If such an effect is demonstrated, the ramifications are potentially quite important. Large differences exist in the sulfur content of plates, forgings and welds. In general, the allowable sulfur levels of plate material are higher than those of forgings, as seen by the ASTM specifications in Table 6. It is also important to note that the maximum allowable level of sulfur in both plates and forgings has recently been reduced to 0.015 wt. percent, for reactor vessel beltline materials. In general, the levels have decreased in recent years, as suppliers aim for increased fracture toughness properties. Therefore, it might be expected that susceptibility to environmentally assisted crack growth would be lower on steels fabricated recently.

If susceptibility is proportional to the manganese sulfide inclusions, it is possible that wide variations in susceptibility could exist in plates of high sulfur content as reported on the material test certificate. This is because the sulfides tend to be concentrated in the upper center of the ingot during solidification, and the rolling process does not redistribute them significantly. Therefore, there could be areas of both high and low susceptibility in such a plate. In forgings the likelihood of this happening is less, because the sulfur level is lower in general to begin with, and the manufacturing process generally results in removal of the center of the ingot and more uniform working of the steel. The sulfide content of a weld is likely to be quite uniform also, particularly those made with an automatic process.

ENVIRONMENTAL CHARACTERIZATION

The level of oxygen in the simulated PWR environment used for crack growth rate testing has recently been a subject of considerable discussion. Therefore, it is important to discuss both the environment of the tests and the actual operating PWR water chemistry.

The specifications for PWR water chemistry for operating plants is given in Table 7. The actual operational chemistry is not remarkably different from that specified with one exception - the oxygen level. The dissolved oxygen in an operating PWR primary water system is actually much lower than the specification. In fact, it is lower than 1 part per billion (ppb), simply because of the operational characteristics of the system.

Therefore, to model the actual PWR system chemistry, the specification of Table 7 can be used as a guide, with the additional requirement that oxygen be as low as possible. The oxygen levels actually measured in Westinghouse Laboratory autoclaves are less than five ppb, which is the limit of resolution of the measurement method, the indigo-carmen bath sample. This low oxygen level is produced by bubbling helium through the system for about two hours, after which the water is circulated through the system overnight before starting to cyclically load the specimen in the morning. The helium bubbling brings the dissolved oxygen level to about 100 ppb, and the recirculating system causes the steel present to scavenge the remaining oxygen overnight.

FRACTOGRAPHY

Efforts in this area have been concentrated on examination of the fracture surfaces of the specimens of the submerged arc weld made with Linde 80 flux and the associated heat-affected zone. Fatigue crack growth rate results from these materials were reported previously [34] and showed a remarkable difference in behavior which appeared to result from different loading forms as illustrated in Figs. 25 and 26. Specifically, crack growth rates in the water environment were much more enhanced under a sinusoidal loading form than under a similarly timed ramp and reset condition. This behavior was found for both high and low R-ratio tests and in both the weld and heat-affected zones. This effect of loading form was not found on all steels tested, so it is of interest to identify any differences which may exist in the fracture surfaces.

Examination of the fracture surfaces from both high and low R ratio tests of the weld showed no unusual features, but clearly the fracture surfaces were much more heavily corroded in the specimens tested under sinusoidal loadings. The same result was found for heat-affected zone specimens which were compared. It is interesting

TABLE 7 - Make-up Water Chemistry - Pressurized Water Reactor

Electrical Conductivity	< 20 μmhos/cm at 25°C
pH	5 to 9
Oxygen	< 0.10 ppm
Chloride	< 0.15 ppm
Fluoride	< 0.15 ppm
Total Solids	< 0.5 ppm
Carbon Dioxide	< 2.0 ppm
Particulates	Filtered to < 25 microns
Silica	< 0.2 ppm
Li^7 OH	1×10^{-4} molal Li (∿ 0.68 ppm Li^7)
Boric Acid	Variable (0 for pH = 9) (∿ 1500 ppm B for pH = 5)
Hydrogen	25 to 35 cc/kg H_2O

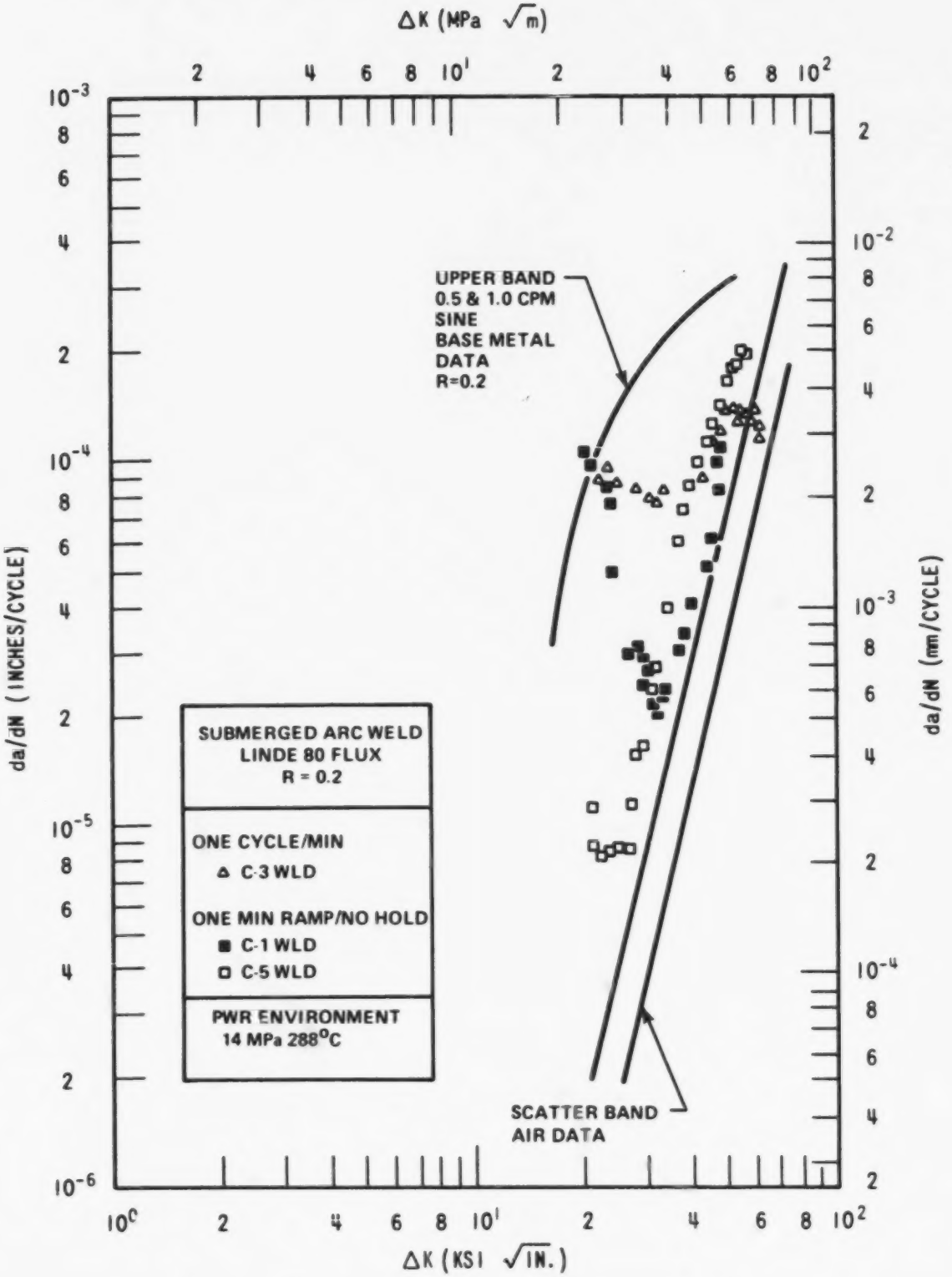

Fig. 25 - Summary of results, Linde 80 welds, R = 0.2.

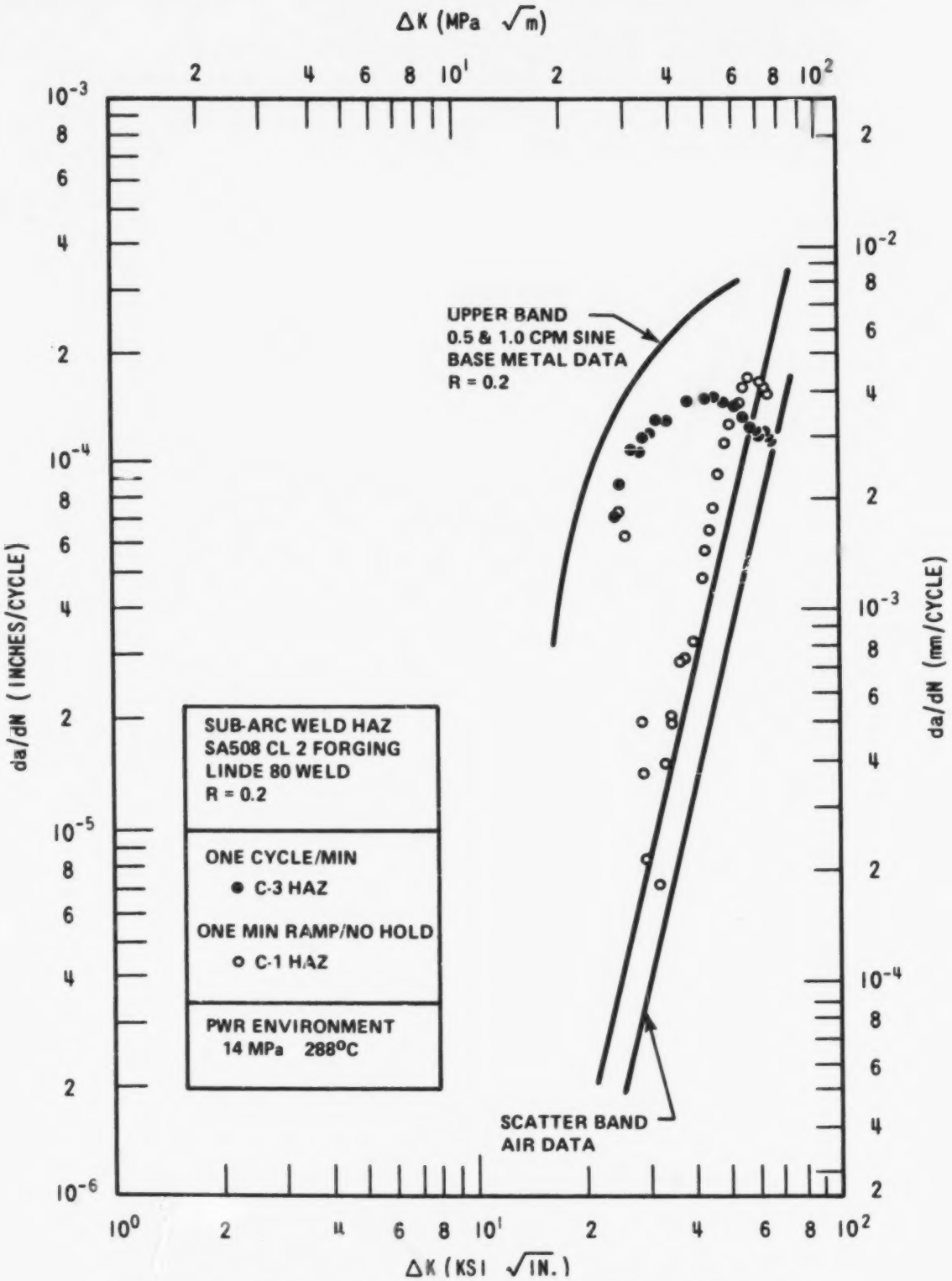
ΔK (MPa √m)
2 4 6 8 10¹ 2 4 6 8 10²
10⁻³ 8 6 4 2 10⁻⁴ 8 6 4 2 10⁻⁵ 8 6 4 2 10⁻⁶
2 4 6 8 10⁻² 8 6 4 2 10⁻³ 8 6 4 2 10⁻⁴ 8 6 4 2
da/dN (INCHES/CYCLE)
da/dN (mm/CYCLE)
UPPER BAND
0.5 & 1.0 CPM SINE
BASE METAL DATA
R = 0.2
SUB-ARC WELD HAZ
SA508 CL 2 FORGING
LINDE 80 WELD
R = 0.2
ONE CYCLE/MIN
● C-3 HAZ
ONE MIN RAMP/NO HOLD
○ C-1 HAZ
PWR ENVIRONMENT
14 MPa 288°C
SCATTER BAND
AIR DATA
10⁰ 2 4 6 8 10¹ 2 4 6 8 10²
ΔK (KSI √IN.)

Fig. 26 - Crack growth rate behavior of Linde 80 weld HAZ, R = 0.2.

that the sinusoidal loading consistently produced more corrosion, even when the test required only one-third as long as a ramp-reset specimen tested under the same conditions. No explanation for this behavior is presently evident, but investigations are continuing.

CONSTANT LOAD K_{Iscc} TESTING

Testing continued on bolt-loaded specimens cut from a forging, from plate, and from two welds and their associated heat-affected zones. Thus far, cracking has only occurred in the heat-affected zone specimens, and the crack propagation has not progressed beyond that reported in the previous progress report [35].

Specimens have been machined from two other weld heat-affected zones and will be inserted into testing chambers during the next reporting period. Further, several of the cracked specimens will be examined fractographically during the next period.

III. RADIATION SENSITIVITY AND POSTIRRADIATION PROPERTIES RECOVERY

A. Evaluation and Comparison of IAEA Coordinated Program Steels and Welds With 288°C Irradiation

J.R. Hawthorne

BACKGROUND

The International Working Group on Reliability of Reactor Pressure Components (IWG-RRPC), sponsored by the International Atomic Energy Agency (IAEA), is conducting a coordinated study on the radiation embrittlement behavior of pressure vessel steels [36]. A primary goal of the program is to assess the radiation behavior of improved steels produced in various countries with the intent of demonstrating that a careful specification of reactor steels can eliminate the problem of potential failure including that caused by neutron irradiation and to demonstrate that knowledge has advanced to the point where steel manufacture and welding technology can routinely produce steel vessels of high radiation resistance [36].

The IWG-RRPC study encompasses plates, forgings and welds produced by the Federal Republic of Germany (FRG), France and Japan and a reference pressure vessel steel plate produced in the United States. The interests of NRL as a program participant include determination of the irradiation characteristics of overseas steel production, the relative radiation resistance of USA versus non-USA steel production, and the correlation of C_v notch ductility, fracture toughness, and strength changes produced by irradiation. Projected results will be of significant value to NRC Regulatory Guide 1.99 for foreign steel evaluations and to vessel construction codes since foreign steels have been employed extensively in some USA reactor vessels.

NRL radiation assessments of four materials supplied by Japan to the IWG-RRPC study have been reported [9]. High radiation resistance was generally observed. Radiation resistance determinations are being made using standard Charpy-V (C_v) and fatigue precracked Charpy-V (PCC_v) tests for notch ductility and dynamic fracture toughness (K_J) respectively.

PROGRESS

During this reporting period, unirradiated condition PCC_v tests were completed for the program materials supplied by France (material codes FP, FF, FW) and the FRG (material code GW). The experimental results are shown in Figs. 27 through 30 and are summarized in Table 8. As before, the determinations for K_J were based on energy absorbed to maximum load corrected for specimen and test machine compliance. EPRI procedures for K_J determinations were satisfied [29] and are summarized in Table 8. Table 8 also lists C_v 41J and C_v 68J transition temperatures determined earlier [13]. Figures 31 to 34 show PCC_v results for the program materials supplied by Japan for additional comparisons. Significant differences in transition temperature but not upper shelf level are found among the materials. It is noted that J-integral determinations on the basis of maximum load imply the absence of stable (rising load) crack extension. Thus, the upper shelf K_J values may overestimate the K_J at crack initiation for these high toughness materials.

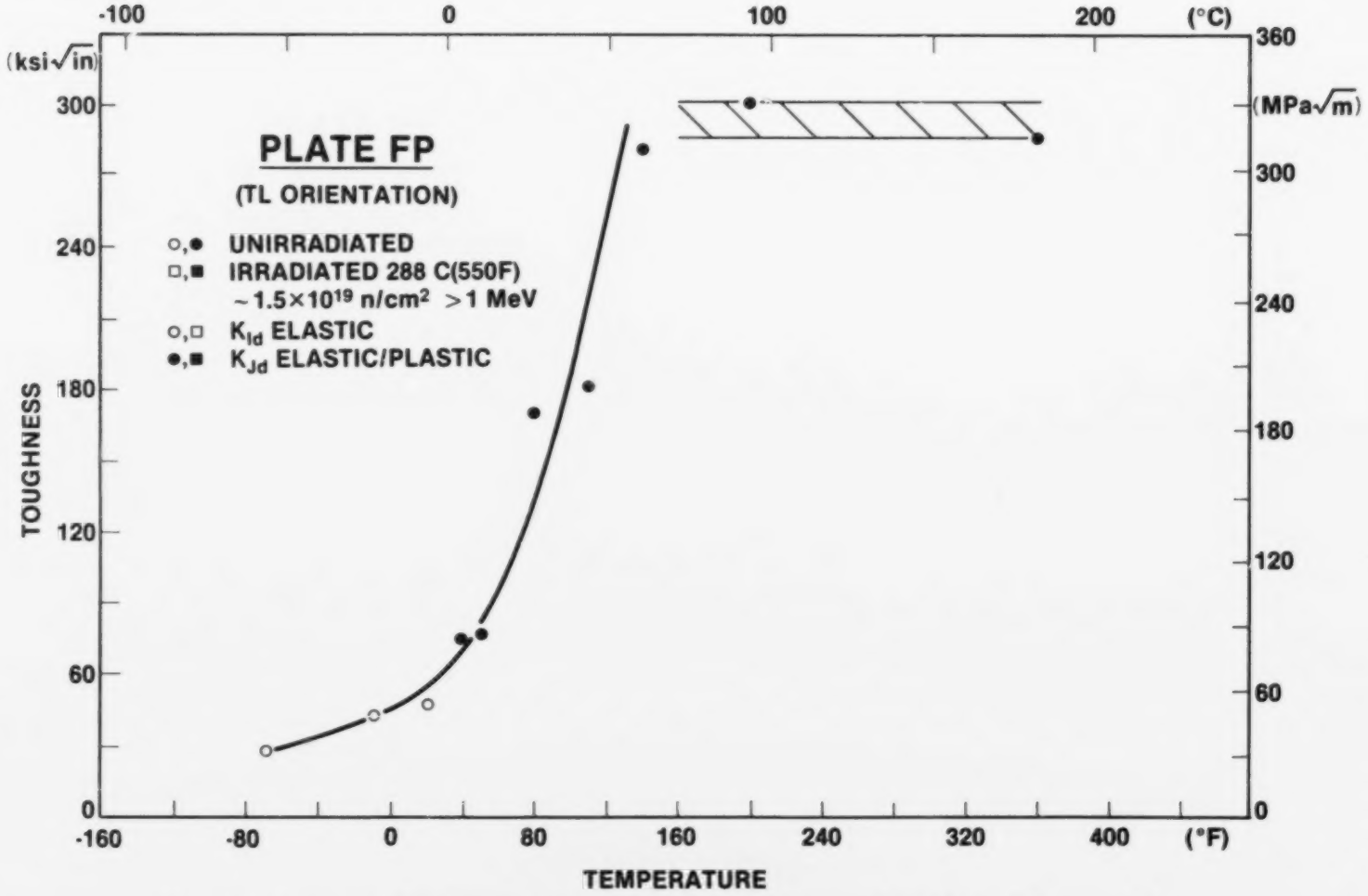

Fig. 27 - Fracture toughness of the A533 Grade B Class 1 plate (Code FP) supplied by France to the IWG-RRPC Program (PCC_V Test Method).

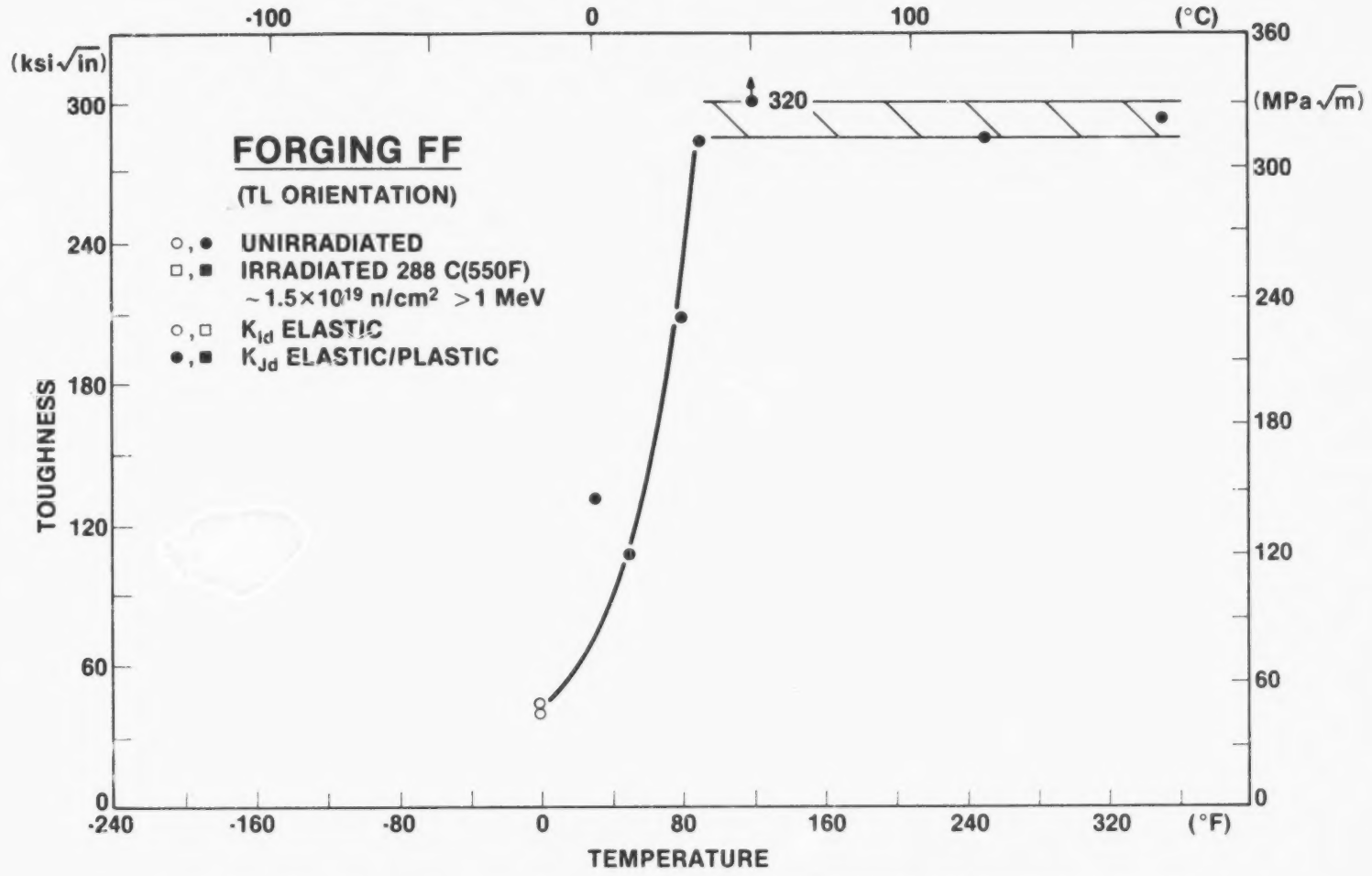

Fig. 28 - Fracture toughness of the A508 Class 3 forging (Code FF) supplied by France to the IWG-RRPC Program.

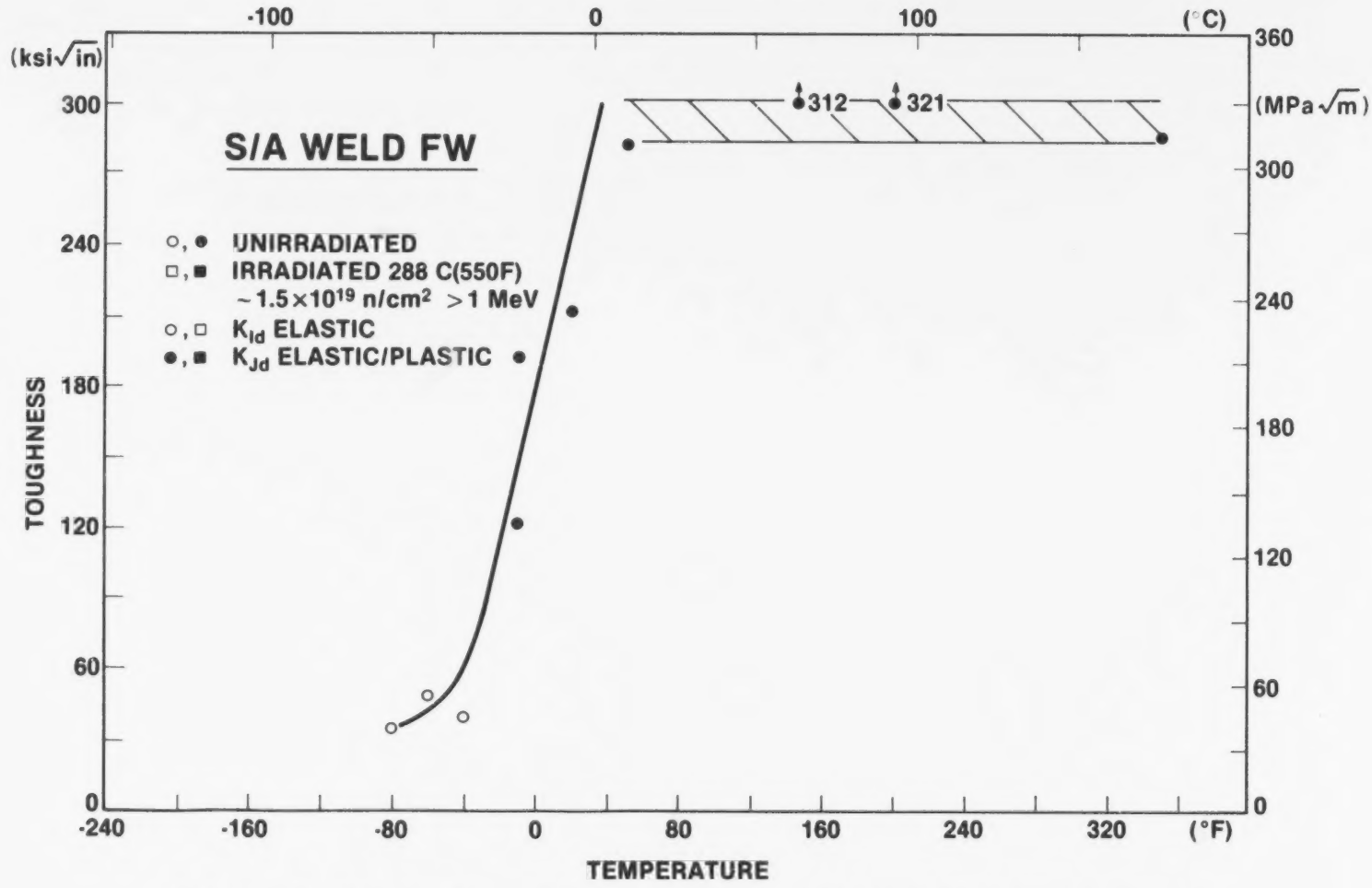

Fig. 29 - Fracture toughness of the submerged arc weld deposit (Code FW) supplied by France to the IWG-RRPC Program.

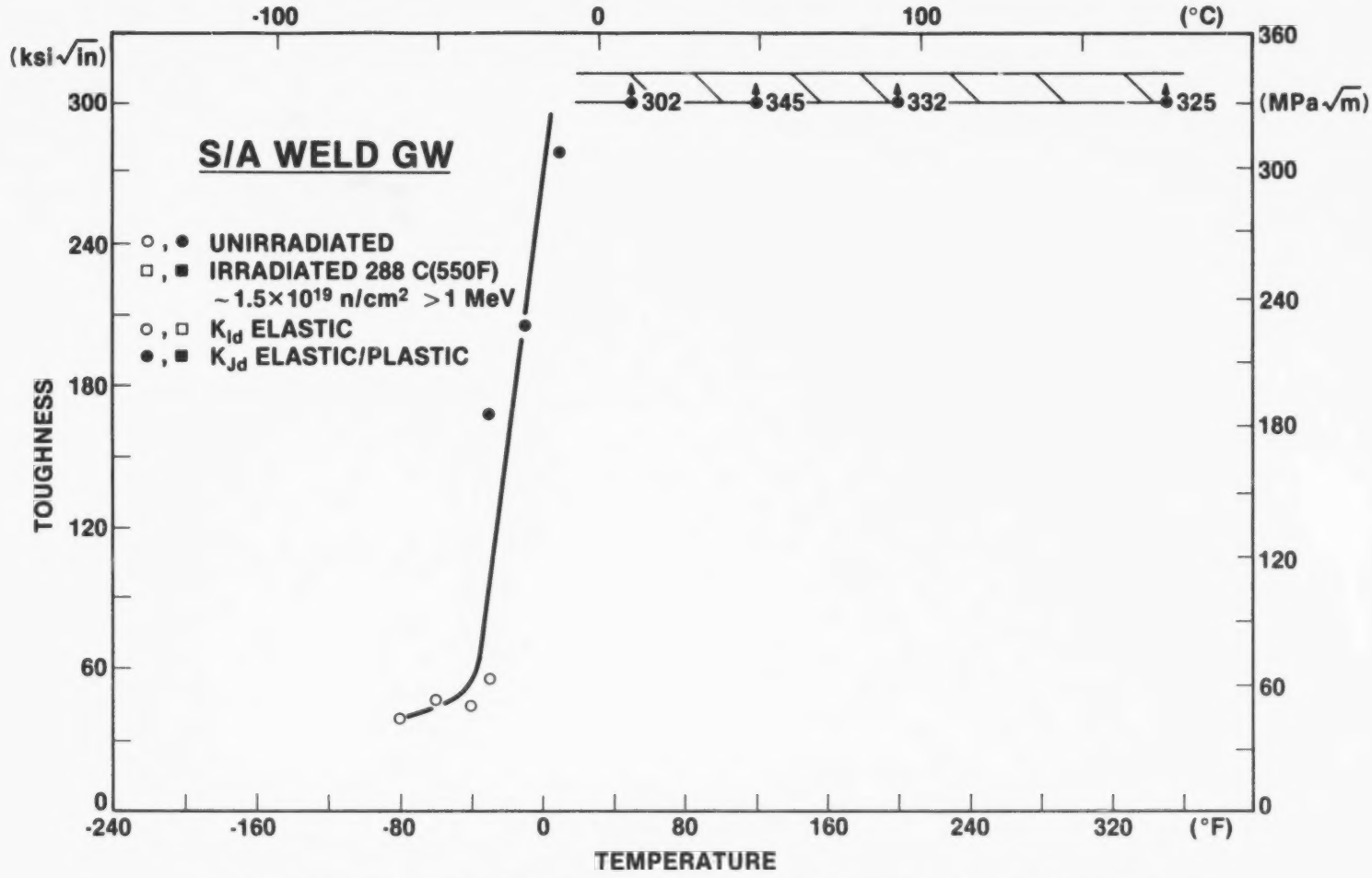

Fig. 30 - Fracture toughness of the submerged arc weld deposit (Code GW) supplied by the FRG to the IWG-RRPC Program.

TABLE 8 - Preirradiation Dynamic Fracture Toughness (K_J) Properties of Program Materials Supplied by France and the FRG.

Material	Source	K_J 100 MPa$\sqrt{m}$ (^oC)	Upper Shelf (MPa$\sqrt{m}$)	C_v 41J (^oC)	C_v 68J (^oC)
Plate, Code FP	France	13	$\geq$315	-18	7
Forging, Code FF	France	4	$\geq$315	$\sim$4	$\sim$35
Weld, Code FW*	France	-34	$\geq$315	-54	-34
Weld, Code GW*	FRG	-34	$\geq$330	-62	-51

*Submerged arc (S/A) process

Additional progress during this period includes completion of the reactor irradiation of the FRG weld deposit. The experiment containing the French materials was disassembled during this period as well.

FUTURE PLANS

Plans for the coming quarter include the initiation of postirradiation C_v and PCC_v tests for the code FP, FF, FW and GW materials and the analysis of neutron dosimeter results.

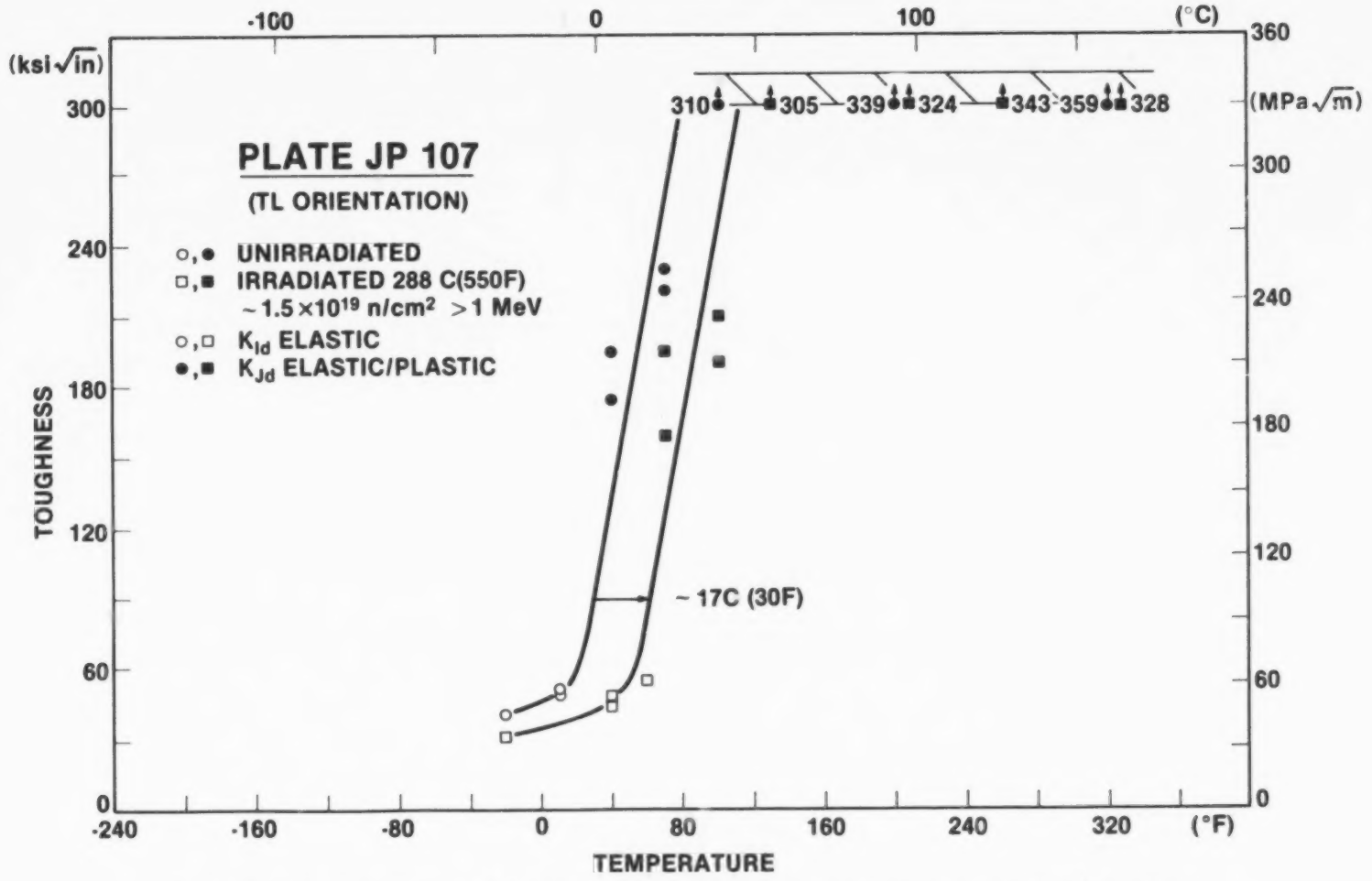

Fig. 31 - Preirradiation and postirradiation fracture toughness of the A533 Grade B plate (Code JP 107) supplied by Japan to the IWG-RRPC Program.

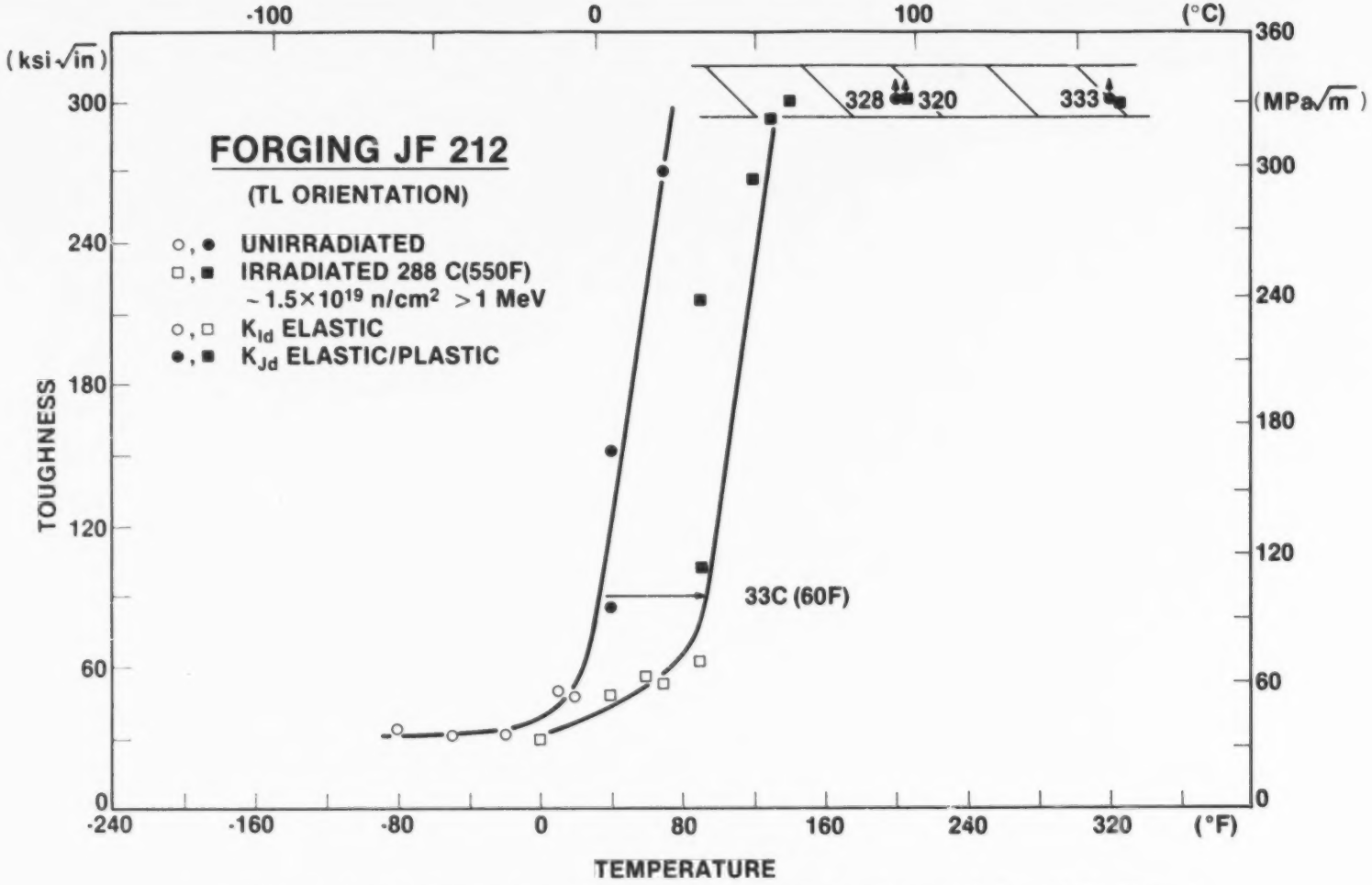

Fig. 32 - Preirradiation and postirradiation fracture toughness of the A508 Class 3 forging (Code JF 212) supplied by Japan to the IWG-RRPC Program.

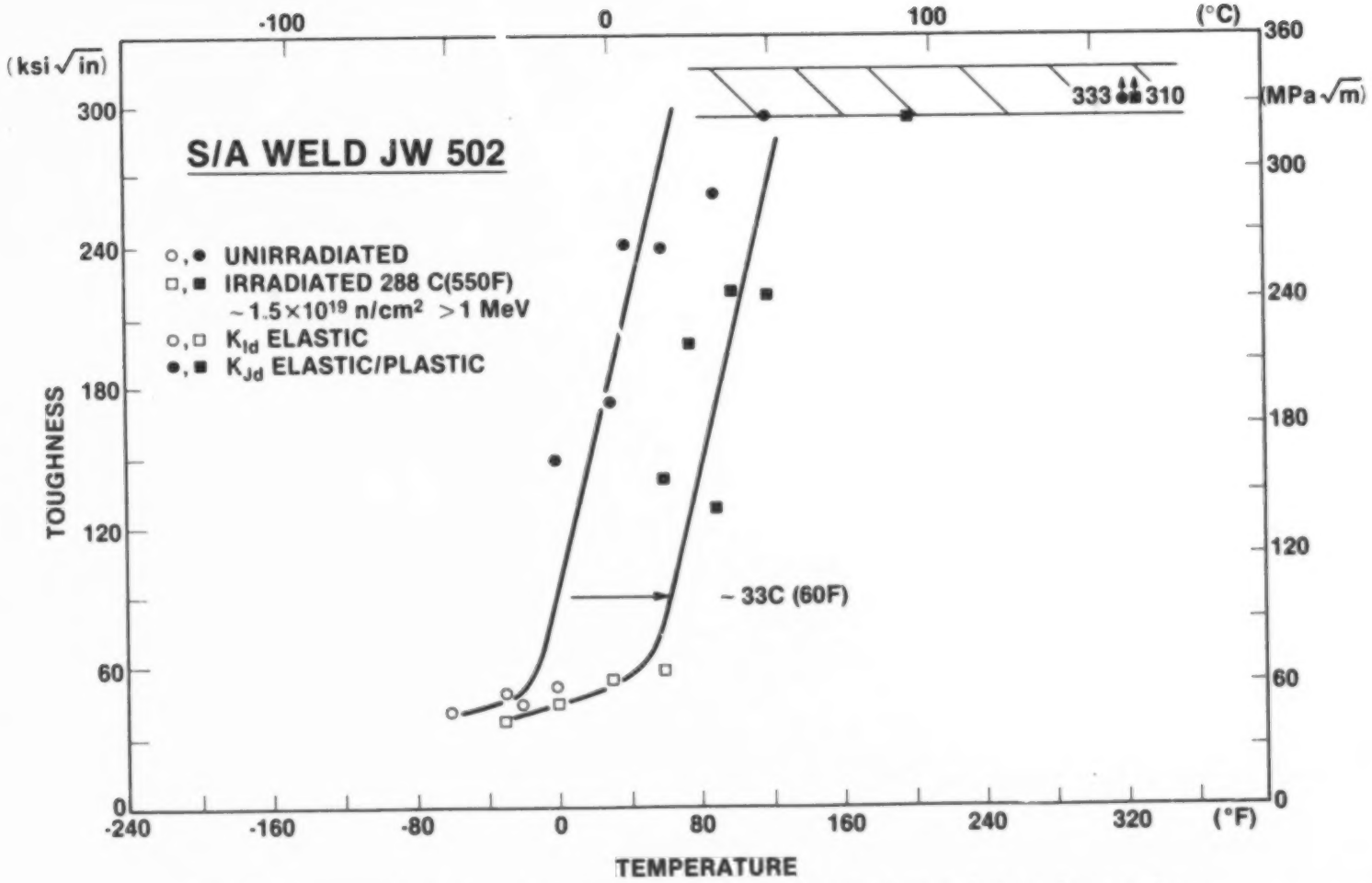

Fig. 33 - Preirradiation and postirradiation fracture toughness of the submerged arc weld deposit (Code JW 502) supplied by Japan to the IWG-RRPC Program.

BLANK PAGE

BLANK PAGE

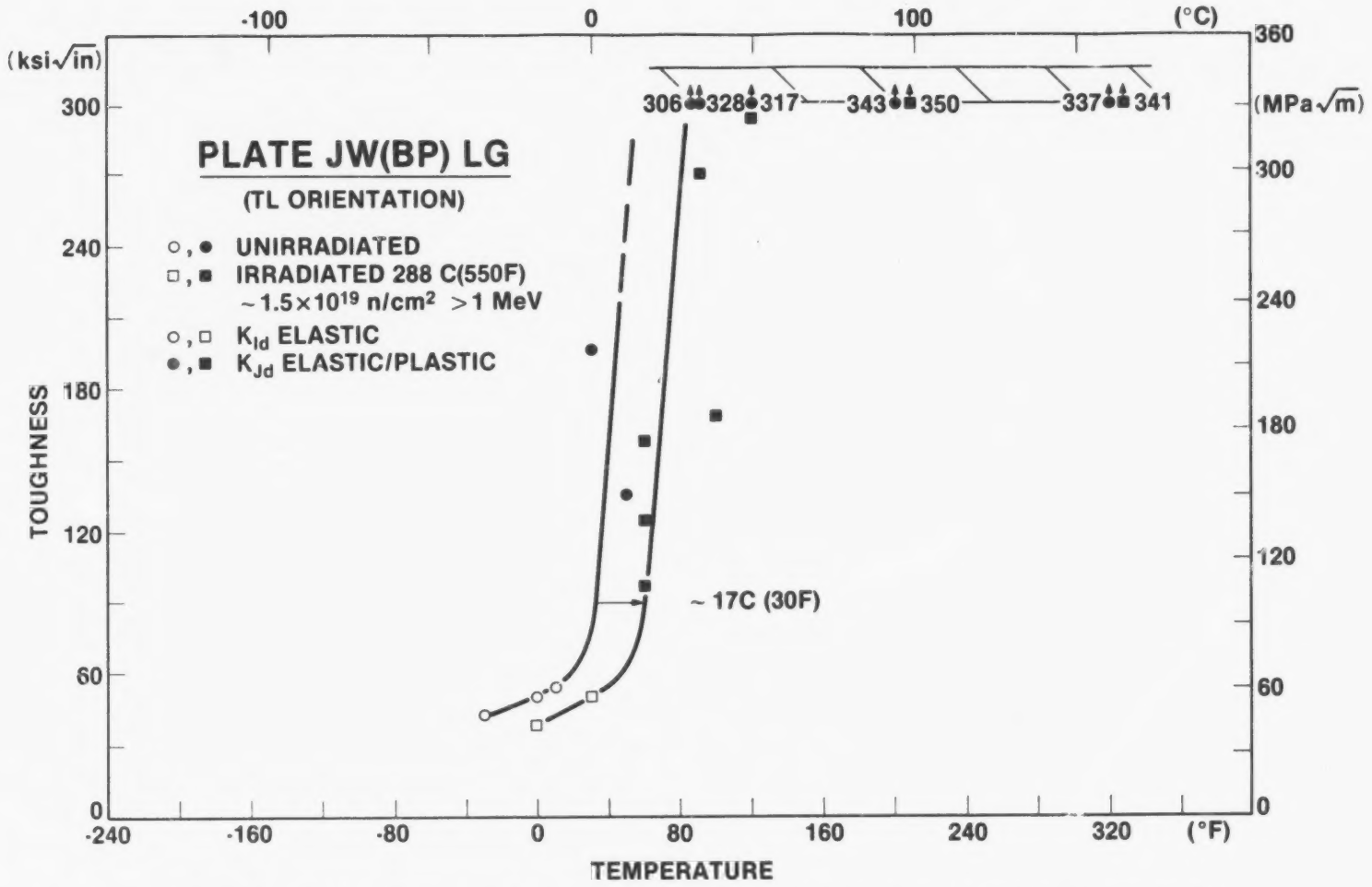

Fig. 34 - Preirradiation and postirradiation fracture toughness of the A533 Grade B plate (Code LG) produced by Japan and supplied as the parent plate for weld JW 502. (See Figure 33).

B. Radiation Resistance of A508 Class 2 Forging Steels

J.R. Hawthorne

BACKGROUND

A significant body of experimental data exists which shows the detrimental effect of 288°C irradiation on the fracture resistance of A302-B and A533-B steel plates. In contrast, only limited data have been developed for the irradiated condition of A508 Class 2 and A508 Class 3 forging steels. Almost all commercial reactor pressure vessels now in service (or under construction) have been fabricated from one of these four steel types. Accordingly, a need exists for a data base which defines the radiation embrittlement trend for A508 forgings for the fluence range of interest and more importantly, which shows the extent of variable sensitivity to irradiation which is possible for this group of materials.

Existing postirradiation data for A508 Class 2 forgings in general suggest that this material has a lower radiation sensitivity than A302-B or A533-B plate steels. For the latter materials, data from postirradiation dynamic tear test and drop weight tests are available to confirm the C_v test indications. Similar independent confirmations of C_v test indications for A508 forgings by-in-large are not yet available.

Objectives of the present investigation are to expand the current data base for A508 Class 2 forgings and to obtain an independent test of their radiation resistance by comparing notch ductility and fracture toughness changes with 288°C neutron exposure. A series of forgings from commercial production were obtained for the study. Fatigue precracked C_v specimens (PCC_v) are being used for dynamic fracture toughness (K_J) determinations wherein K_J values are based on specimen energy absorption to maximum load as discussed in the preceding section. Compact tension (CT) specimens are also being irradiated for future determinations of static fracture toughness and R-curve characteristics.

PROGRESS

The forging materials have been irradiated at 288°C in two experiments in the 2MW pool reactor of the State University of New York at Buffalo. The target neutron fluence was $\sim 2.5 \times 10^{19}$ n/cm^2, E>1 MeV (calculated spectrum fluence). The first experiment (UB-21) contained C_v and PCC_v specimens of four forgings from separate steel melts; the second experiment (UB-26) contained C_v, tensile and CT specimens of one forging (Code V82) which was chosen on the basis of the initial irradiation results. Postirradiation testing of the V82 forging has been completed (with the exception of CT specimens). The experimental data are presented in Figs. 35 and 36. Postirradiation testing of the remaining three forgings has also been completed; however, unirradiated (reference) condition data are not yet available for property comparisons.

Several observations can be made from Figs. 35 and 36. Overall, the C_v and PCC_v data from experiments 21 and 26 are in generally good agreement and illustrate the reproducibility of results. The fluence for experiment 21 was 2.8×10^{19} n/cm^2; the fluence of experiment 26 has not yet been established but its radiation exposure time was very similar. In Fig. 35, good radiation resistance is indicated by the relatively small C_v transition temperature elevations measured at the 41J and 68J energy levels and by the high C_v upper shelf retention. We note, however, that the respective transition temperature elevations are quite different, that is ≤ 11°C vs 36°C. The preirradiation nil ductility transition (NDT) temperature for this forging determined by

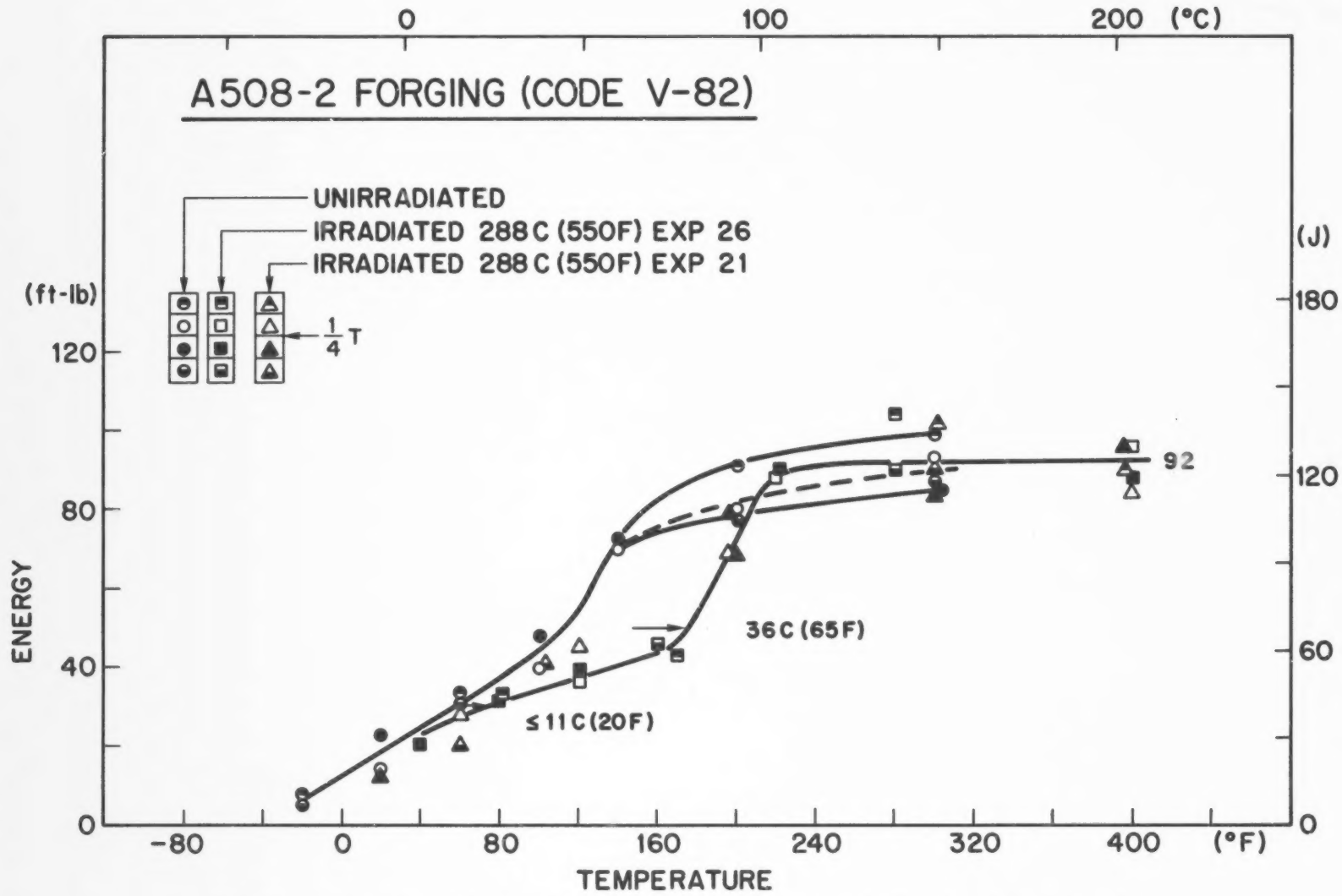

Fig. 35 - Charpy-V notch ductility of forging V82 before and after irradiation to 2.8 x 10^{19} n/cm^2, E >1 MeV. Test results from two reactor experiments are shown.

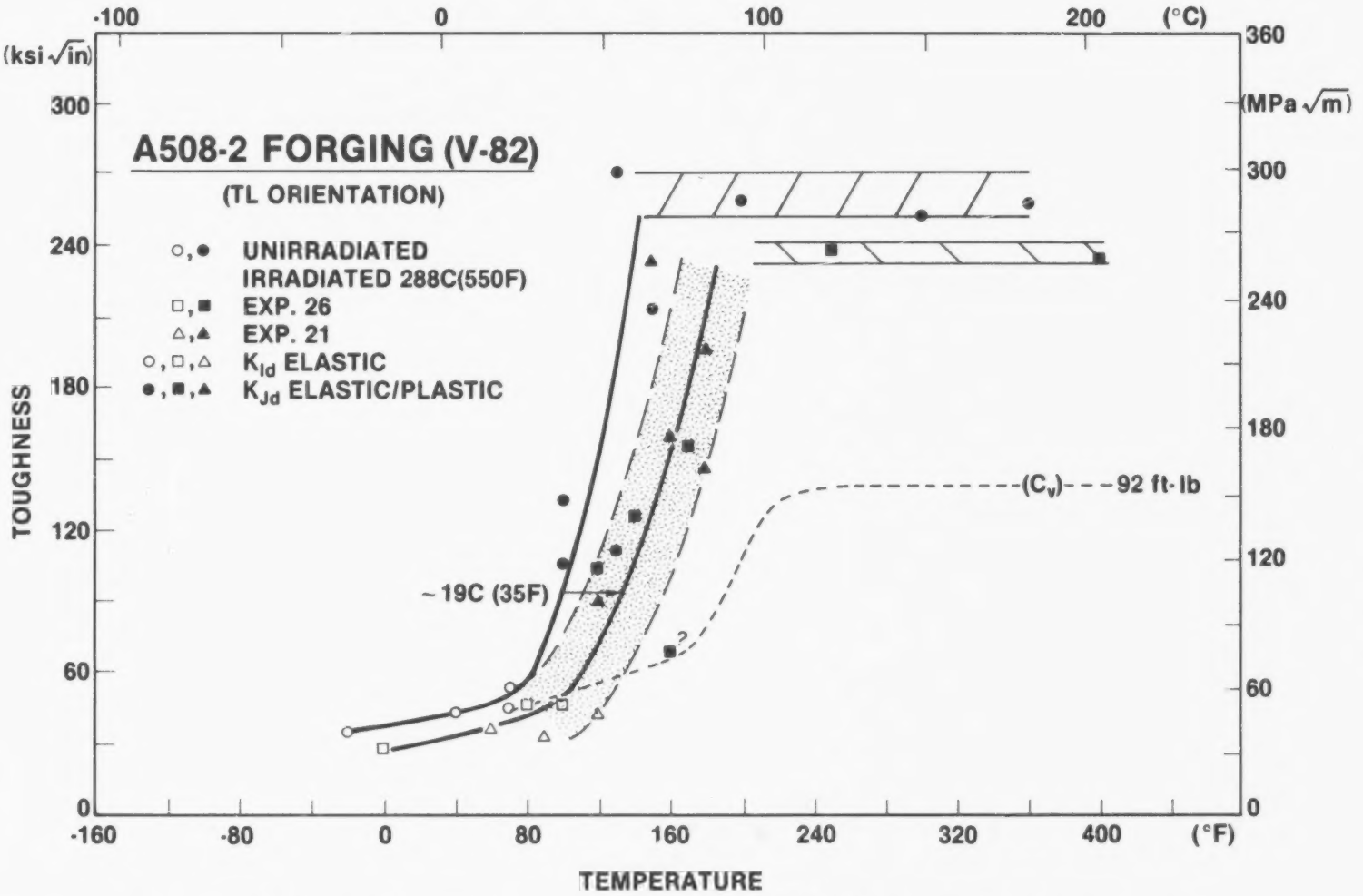

Fig. 36 - Dynamic fracture toughness (PCC_v test method) of forging V82 before and after irradiation to 2.8×10^{19} n/cm^2, E > 1 MeV. The PCC_v specimens and C_v specimens of Fig. 28 were commingled in each reactor experiment during irradiation.

the drop weight test method, was 4°C or 40°F which corresponds to the C_v 34J energy level. In Fig. 36, the PCC_v test results are found to support the C_v findings on forging radiation resistance. Specifically, the radiation-induced elevation in the 100 MPa$\sqrt{m}$ transition is on the order of only 19°C (35°F); the reduction in upper shelf K_J level is also small. Comparing Fig. 36 with Fig. 35, the sharp increase in K_J with temperature is noted to take place at a C_v energy level of about 41J. On the other hand, the C_v energy trend with temperature shows a gradual increase in the range of 25J to 65J. This relationship is under further investigation. Finally, tensile tests revealed very little change in strength or ductility with irradiation. Preirradiation and postirradiation yield strengths at 24°C (single test determinations) were 463 MPa and 481 MPa, respectively; corresponding tensile strengths were 611 MPa and 602 MPa respectively. Preirradiation and postirradiation tensile elongation values for the 25.4 mm gage length were 25.6 and 22.9 percent, respectively. Accordingly, the C_v, PCC_v and tensile property changes are in good agreement on the radiation resistance of this forging.

FUTURE PLANS

Plans for the coming reporting period include completion of reference C_v and PCC_v tests for forgings codes V80, V81 and BCB and the initiation of CT reference tests for forging V82. Material performances will be compared against metallurgical properties in the next report of progress.

REFERENCES

1. G. D. Whitman, "Heavy Section Steel Technology Program, Quarterly Progress Report for July-September 1979," NUREG/CR-1197, Oak Ridge National Laboratory, Oak Ridge, Tn., Oct. 1978.

2. F. J. Loss, Ed., "Structural Integrity of Water Reactor Pressure Boundary Components, Progress Report Ending 31 May 1976," NRL Memorandum Report 3353, Sep. 1976, pp. 15-21.

3. P. C. Paris, H. Tada, A. Zahoor and H. Ernst, "Instability of the Tearing Mode of Elastic-Plastic Crack Growth," in Elastic-Plastic Fracture, ASTM STP 668, American Society for Testing and Materials, Philadelphia, Pa., 1979, pp. 5-36.

4. G. D. Whitman, "Heavy Section Steel Technology Program, Quarterly Progress Report for April-June 1976," ORNL/NUREG/TM-49, Oak Ridge National Laboratory, Oak Ridge, Tn., Oct. 1976, pp. 27-38.

5. R. G. Berggren, "Irradiation Effects," presented to Vessel Integrity Review Group, U. S. Nuclear Regulatory Commission, Silver Spring, MD, 23-24 July 1980.

6. F. J. Loss, Ed., "Structural Integrity of Water Reactor Pressure Boundary Components, Quarterly Progress Report, October-December 1979," NUREG/CR-1268, NRL Memorandum Report 4174, Mar. 20, 1980.

7. J. A. Williams and K. W. Carlson, "Fracture Toughness of Welds 61W, 62W and 63W from Second 4T Irradiations - 0.5TCT Specimen Tests," TC-1520, Hanford Engineering Development Laboratory, Richland, Wa., Sep. 1979.

8. F. J. Loss, Ed., "Structural Integrity of Water Reactor Pressure Boundary Components, Quarterly Progress Report, April-June 1979," NUREG/CR-0943, NRL Memorandum Report 4064, Sep. 28, 1979.

9. F. J. Loss, Ed., "Structural Integrity of Water Reactor Pressure Boundary Components, Annual Report, Fiscal Year 1979," NUREG/CR-1128, NRL Memorandum Report 4122, 31 Dec. 1979.

10. H. Ernst and P. C. Paris, "Techniques of Analysis of Load-Displacement Records by J-Integral Methods," NUREG/CR-1222, U. S. Nuclear Regulatory Commission, Jan. 1980.

11. J. W. Hutchinson and P. C. Paris, "The Theory of Stability Analysis of J-Controlled Crack Growth," Elastic-Plastic Fracture, ASTM STP 668, 1979, pp. 37-64.

12. C. F. Shih, "An Engineering Approach for Examining Crack Growth and Stability in Flawed Structures," Proceedings of CSNI Specialists Meeting in Plastic Tearing Instability, NUREG/CP-0010, U. S. Nuclear Regulatory Commission, Jan 1980.

13. F. J. Loss, Ed., "Structural Integrity of Water Reactor Pressure Boundary Components, Quarterly Progress Report, January-March 1980," NUREG/CR-1472, NRL Memorandum Report 4254, 1 Aug. 1980.

14. W. H. Cullen, R. E. Taylor, H. E. Watson and W. Rohrs, "Evaluation of Critical Factors in Crack Growth Rate Studies" in Structural Integrity of Water Reactor Pressure Boundary Components, Quarterly Progress Report, January-March 1980, NUREG/CR-1472, NRL Memorandum Report 4254, Aug. 1, 1980, pp. 16-36.

15. M. O. Speidel, et al., "Corrosion Fatigue and Stress Corrosion Crack Growth in High-Strength Aluminum Alloys, Magnesium Alloys, and Titanium Alloys Exposed to Aqueous Solutions," in Corrosion Fatigue - Chemistry, Mechanics and Microstructure, NACE-2, National Association of Corrosion Engineers, 1972.

16. W. H. Cullen, et al., "Fatigue Crack Growth of A508-2 Steel in High-Temperature, Pressurized Reactor-Grade Water," NUREG/CR-0969, NRL Memorandum Report 4063, Sep. 28, 1979.

17. W. H. Cullen, H. E. Watson, V. Provenzano, "Results of Cyclic Crack Growth Rate Studies in Pressure Vessel and Piping Steels" in Structural Integrity of Water Reactor Pressure Boundary Components, Annual Report, Fiscal Year, 1979, NUREG/CR-1128 NRL Memorandum Report 4122, Dec. 31, 1979, pp. 43-81.

18. L. W. James, "Fatigue Crack Propagation in Neutron-Irradiated Ferritic Pressure-Vessel Steels," Nuclear Safety, Vol. 18, 1973, pp. 791-801.

19. W. H. Cullen and K. Torronen, "A Review of Fatigue Crack Growth of Pressure Vessel and Piping Steels in High-Temperature, Pressurized Reactor-Grade Water," NRL Memorandum Report 4298, Sep. 19, 1980.

20. R. P. Wei, S. R. Novak, D. P. Williams, "Some Important Considerations in the Development of Stress-Corrosion Cracking Test Methods," Proceedings 33rd AGARD Conference on Structures and Materials, Brussels, Belgium, 1971.

21. P. C. Paris, R. J. Bucci, E. T. Wessel, W. G. Clark and T. R. Mager. "An Extensive Study on Low Fatigue Crack Growth Rates in A533 and A508 Steels," in Stress Analysis and Growth of Cracks, ASTM STP 513, American Society for Testing and Materials, Philadelphia, Pa., 1972, pp. 141-176.

22. W. G. Clark, Jr., "Effect of Temperature and Section Size on Fatigue Crack Growth in Pressure Vessel Steel" J. Materials, Vol. 16, 1971, pp. 134-149.

23. D. K. Sturm, F. J. Loss and W. H. Cullen, "Qualification of Crack Growth Data Beyond ASTM Committee E-24 Criteria", Report of NRL Progress, Sep. 1978, pp. 4-6.

24. W. H. Bamford, D. M. Moon and L. J. Ceschini, "Effect of High-Temperature Primary Reactor-Grade Water on the Subcritical Crack Growth of Reactor Vessel Steel" in HSST Quarterly Progress Report for October-December 1978, ORNL/NUREG/TM-298, Oak Ridge National Laboratory, Oak Ridge, Tn., Apr. 1979, pp. 14-23.

25. M. E. Indig, "Corrosion Potential and CERT Evaluations of Carbon Steel in BWR Environments" in BWR Environmental Cracking Margins for Carbon Steel Piping - First Semiannual Progress Report, July 1978 to December 1979, General Electric Report, NEDC-24625, Jan. 1979.

26. R. N. Parkins, "Stress Corrosion Spectrum", British Corrosion Journal, Vol. 7, pp. 15-28, 1972.

27. F. P. Ford and M. Silverman, "Mechanistic Aspects of Environment-Controlled Crack Propagation in Steel/Aqueous Environment Systems", HTGE-451-8-12, General Electric Company, May 1979.

28. ASTM Book of Standards, Part 4, American Society for Testing and Materials, Philadelphia, PA, 1980.

29. ASME Boiler and Pressure Vessel Code, Section II, Material Specifications, American Society of Mechanical Engineers, New York, N.Y., 1977, pp. 308-309.

30. A. D. Wilson, "Fatigue Crack Propagation in A533-B Steels," Trans. ASME, J. Pressure Vessel Technology, American Society of Mechanical Engineers, New York, N.Y., August 1977, p. 459.

31. A. D. Wilson, "Fatigue Crack Propagation in A533-B Steels - Metallographic and Fractographic Analyses," Trans. ASME, J. Pressure Vessel Technology, American Society of Mechanical Engineers, New York, N.Y., May 1979, p. 155.

32. W. H. Bamford and D. M. Moon, "Some Mechanistic Observations on the Crack Growth Characteristics of Pressure Vessel and Piping Steels in PWR Environment," Corrosion, June 1980.

33. G. Slama, Framatome, Paris, France, personal correspondence, May 1980.

34. W. H. Bamford, et. al, "Cyclic Crack Growth Rate Studies," NUREG/CR-1268, NRL Memorandum Report 4174, Mar. 20, 1980, p. 37.

35. W. H. Bamford, et. al, "Corrosion Fatigue Crack Growth Behavior of Pressure Vessel Steels," NUREG/CR-1474, NRL Memorandum Report 4254, Aug. 1, 1980, p. 37-39.

36. "Coordinated Research Programme on Analyses of the Behavior of Advanced Reactor Pressure Vessel Steels Under Neutron Irradiation," Proceedings, IWG-RRPC-78/3, Vienna, Austria, 17-18 Oct 1977.

37. D. R. Ireland, W. L. Server, R. A. Wullaert, "Procedures for Testing and Data Analysis," ETI Technical Report 75-43, Task-A Topical Report, Effects Technology, Inc., Santa Barbara, Ca., Oct. 1975.